Molecular Neurobiology (2024) 61:2496–2513
https://doi.org/10.1007/s12035-023-03718-9

In Vivo Intracerebral Administration of α-Ketoisocaproic Acid to Neonate Rats Disrupts Brain Redox Homeostasis and Promotes Neuronal Death, Glial Reactivity, and Myelination Injury

Ângela Beatris Zemniaçak[1] · Rafael Teixeira Ribeiro[1] · Camila Vieira Pinheiro[1] · Sâmela de Azevedo Cunha[1] · Tailine Quevedo Tavares[1] · Ediandra Tissot Castro[1] · Guilhian Leipnitz[1,2] · Moacir Wajner[1,2,3] · Alexandre Umpierrez Amaral[1,4]

Received: 27 August 2023 / Accepted: 17 October 2023 / Published online: 1 November 2023

Abstract

Maple syrup urine disease (MSUD) is caused by severe deficiency of branched-chain α-keto acid dehydrogenase complex activity, resulting in tissue accumulation of branched-chain α-keto acids and amino acids, particularly α-ketoisocaproic acid (KIC) and leucine. Affected patients regularly manifest with acute episodes of encephalopathy including seizures, coma, and potentially fatal brain edema during the newborn period. The present work investigated the ex vivo effects of a single intracerebroventricular injection of KIC to neonate rats on redox homeostasis and neurochemical markers of neuronal viability (neuronal nuclear protein (NeuN)), astrogliosis (glial fibrillary acidic protein (GFAP)), and myelination (myelin basic protein (MBP) and 2′,3′-cyclic-nucleotide 3′-phosphodiesterase (CNPase)) in the cerebral cortex and striatum. KIC significantly disturbed redox homeostasis in these brain structures 6 h after injection, as observed by increased 2',7'-dichlorofluorescein oxidation (reactive oxygen species generation), malondialdehyde levels (lipid oxidative damage), and carbonyl formation (protein oxidative damage), besides impairing the antioxidant defenses (diminished levels of reduced glutathione and altered glutathione peroxidase, glutathione reductase, and superoxide dismutase activities) in both cerebral structures. Noteworthy, the antioxidants N-acetylcysteine and melatonin attenuated or normalized most of the KIC-induced effects on redox homeostasis. Furthermore, a reduction of NeuN, MBP, and CNPase, and an increase of GFAP levels were observed at postnatal day 15, suggesting neuronal loss, myelination injury, and astrocyte reactivity, respectively. Our data indicate that disruption of redox homeostasis, associated with neural damage caused by acute intracerebral accumulation of KIC in the neonatal period may contribute to the neuropathology characteristic of MSUD patients.

Keywords Maple syrup urine disease · α-Ketoisocaproic acid · Cerebral cortex · Striatum · Redox homeostasis · Neurochemical markers

Abbreviations

ANOVA	One-way analysis of variance
BCAA	Branched-chain amino acids
BCKA	Branched-chain α-keto acids
BCKDH	Branched-chain α-keto acid dehydrogenase
CNPase	2′,3′-Cyclic-nucleotide 3′-phosphodiesterase
DCFH	2',7'-Dichlorofluorescein

✉ Alexandre Umpierrez Amaral
alexandreamaral@uricer.edu.br

[1] Programa de Pós-Graduação em Ciências Biológicas: Bioquímica, Instituto de Ciências Básicas da Saúde, Universidade Federal do Rio Grande do Sul, Porto Alegre, RS, Brazil

[2] Departamento de Bioquímica, Instituto de Ciências Básicas da Saúde, Universidade Federal do Rio Grande do Sul, Porto Alegre, RS, Brazil

[3] Serviço de Genética Médica, Hospital de Clínicas de Porto Alegre, Porto Alegre, RS, Brazil

[4] Programa de Pós-Graduação em Atenção Integral à Saúde, Universidade Regional Integrada do Alto Uruguai e das Missões, Avenida Sete de Setembro, 1621, Erechim, RS 99709-910, Brazil

GFAP	Glial fibrillary acidic protein
GPx	Glutathione peroxidase
GR	Glutathione reductase
GSH	Reduced glutathione
GSSG	Oxidized glutathione
HO-1	Heme oxygenase-1
icv	Intracerebroventricular
KIC	α-Ketoisocaproic acid
MDA	Malondialdehyde
MEL	Melatonin
MCT/SLC16A1	Monocarboxylate transporter
MSUD	Maple syrup urine disease
MBP	Myelin basic protein
NAC	N-Acetylcysteine
NeuN	Neuronal nuclear protein
Nrf2	Nuclear factor erythroid 2-related factor 2
PBS	Phosphate-buffered saline
PND	Postnatal day
RNS	Reactive nitrogen species
ROS	Reactive oxygen species
SOD	Superoxide dismutase
TCA	Trichloroacetic acid

Introduction

Maple syrup urine disease (MSUD) (MIM 248600) is an autosomal recessive inherited disorder, with a worldwide incidence of 1:185,000 live births. It is caused by defects of the branched-chain α-ketoacid dehydrogenase (BCKDH, EC 1.2.4.4) complex, leading to accumulation in tissues and biological fluids of the branched-chain α-keto acids (BCKA), α-ketoisocaproic acid (KIC), α-keto-β-methylvaleric acid, and α-ketoisovaleric acid, and the equivalent amino acids leucine, isoleucine, and valine [1, 2]. MSUD is classified into four genetic variants, the classic, the intermediate, the intermittent, and the thiamine-responsive forms [1]. The classical form is the most severe, presenting during the neonatal period, sometimes called neonatal MSUD [3, 4].

Patients with classical neonatal MSUD usually manifest with nonspecific signs of metabolic intoxication, such as irritability, somnolence, anorexia, vomiting, dehydration, and ketoacidosis, which is followed by neurological symptoms, such as lethargy, coma, apnea, opisthotonos, and cytotoxic cerebral edema. Later in infancy or childhood, they develop physical and psychomotor delay with intellectual disability and movements disorders such as dystonia and tremor [1, 2]. Neuropathological findings comprise hypomyelination and cytotoxic edema in various brain areas, including the basal ganglia and cerebral cortex [5–7], and brain atrophy [8, 9]. Noteworthy, MSUD is considered an intoxicating inherited disorder in which KIC and leucine are the main neurotoxic metabolites, once augmented plasma concentrations of these compounds are associated with the appearance or worsening of the neurological symptoms that take place during crises of metabolic decompensation accompanied by excessive proteolysis [1, 2]. Although various mechanisms have been proposed to explain the cerebral damage in MSUD, the exact underlying pathophysiological mechanisms are still poorly known.

Regarding the BCKA, intracerebroventricular (icv) administration of KIC to adult (60-day-old) or young (30-day-old) rats was shown to cause learning deficits and behavioral changes [10]. KIC icv injection was also shown to induce oxidative damage to biomolecules [11], decrease of brain-derived neurotrophic factor and nerve growth factor levels [12], as well as of the activities of the respiratory chain complexes I and II-III [13] in different cerebral regions. KIC was also shown to alter the levels of interferon-γ and tumor necrosis factor-α [14].

Furthermore, in vitro exposition of brain to the BCKA, particularly to KIC, caused lipid oxidative damage and impairment of the antioxidant defenses [15, 16], as well as inhibition of α-ketoglutarate dehydrogenase and pyruvate dehydrogenase activities [17, 18]. KIC also reduced oxygen consumption in state 3 respiration and disrupted mitochondrial membrane potential [19]. Another work showed that the BCKA accumulating in MSUD inhibit CO_2 formation and increase lactate release in the brain of young rats [20].

On the other hand, several studies revealed that in vivo and in vitro exposition of rat brain to the BCAA induce oxidative stress through lipid peroxidation, DNA, and protein damage, and altered activities of antioxidant enzymes [21–24]. BCAA also decreased CO_2 production and the activities of creatine kinase, and respiratory chain complexes II–III, III, and IV [18, 25, 26]. Of note, lipid and protein oxidative damage was found in the plasma of MSUD patients [27–30], corroborating the investigations with the chemical animal models of this disease. Noteworthy, all these previous studies designed to clarify MSUD pathogenesis were performed in the brain of young or adult rats, whereas the onset of the neurological findings in MSUD patients is usually manifested in the first few days of life. Therefore, further studies using neonatal brain are necessary to clarify the pathophysiology of the brain damage in this disease.

Therefore, since to the best of our knowledge, there were no reports on the deleterious effects of KIC on brain functioning in early days of development, the present work evaluated the ex vivo effects of intracerebral administration of KIC to neonate rats on redox homeostasis, as well as on neuropathological landmarks in the cerebral cortex and striatum. The antioxidants N-acetylcysteine (NAC) and melatonin (MEL) were used in some experiments to evaluate their neuroprotective effects on redox homeostasis.

Material and Methods

Animals and Reagents

A total of 84 1-day-old (neonate) Wistar rats from Centro de Reprodução e Experimentação de Animais de Laboratório (CREAL) at the Federal University of Rio Grande do Sul (UFRGS), Porto Alegre, Brazil, were used in this work. The newborn rats were kept with their dam on a 12:12-h light/dark cycle at temperature of 22 ± 1 °C. Free water and commercial chow with 20% (w/w) protein were available to dams.

All reagents were purchased from Merck (St. Louis, MO, USA). On the day of the experiments, KIC, MEL, and NAC solutions were made, and the pH adjusted to 7.4.

icv Injection of KIC

A schematic representation of the experimental design is shown in Fig. 1. Neonate rats were submitted to an icv injection of KIC (1 µmol/g body weight, dissolved in 0.01 M phosphate-buffered saline (PBS), pH 7.4, in a volume of 0.5 µL/g body weight), or an equal volume of 0.01 M PBS, pH 7.4 (control), into the cisterna magna, as previously described [31, 32]. After recovering in a heating pad at 37 °C, neonate animals returned to their dam until euthanasia that was immediately followed by the various analyses. In some experiments, neonatal rats were pre-treated with two intraperitoneal injections (volume of 2 µL/g body weight) of NAC (300 mg/kg and 400 mg/kg, respectively) or MEL (40 mg/kg, each) 24 and 1 h prior to KIC icv administration [32, 33]. The animals were then euthanized at 6 h after KIC icv infusion to evaluate redox homeostasis parameters and heme oxygenase-1 (HO-1) protein immunocontent, at postnatal day (PND) 7 to determine oxidative stress measures, or at PND 15 for the immunofluorescence analyses. It is stressed that the neonates were randomly distributed into the various experimental groups, the researchers that conducted the experimental procedures did not know which solution was administered to the animals (PBS, KIC, NAC, or MEL), and the groups were not identified during the analyses. The sample size and power calculations for the biochemical assays, Western blotting, and immunofluorescence analysis utilized the software Minitab 16, and considered the following parameters: standard deviation of 10%, power of 0.9, difference of 25%, and 2 or 3 levels (experimental groups). These parameters were based on previous reports from our and other research groups [32, 34, 35].

Parameters of Redox Homeostasis

Preparation of Tissue Homogenates

The animals were euthanized by decapitation, the brain removed, and the cerebral cortex and striatum dissected. These cerebral structures were then homogenized (1:10) in 20 mM sodium phosphate buffer, pH 7.4, with 140 mM KCl, centrifuged at 800 *g* and the supernatants used for the determination of redox homeostasis parameters, excepting for the nitrate and nitrite levels that were measured with the forebrain supernatants.

2',7'-Dichlorofluorescein (DCFH) Oxidation

Reactive oxygen species (ROS) production was measured by DCFH oxidation, as described by LeBel et al. [36]. Tissue homogenates were incubated for 30 min at 37 °C with the cell-permeant diacetate form (DCF-DA), which is cleaved to generate DCFH that is oxidized by ROS to form the fluorescent product DCF. Fluorescence was measured in a Spectramax M5 at 480 nm (excitation) and 535 nm (emission). A standard curve was carried out with DCF (0–10 µM) and the data expressed as µmol DCF per milligram protein.

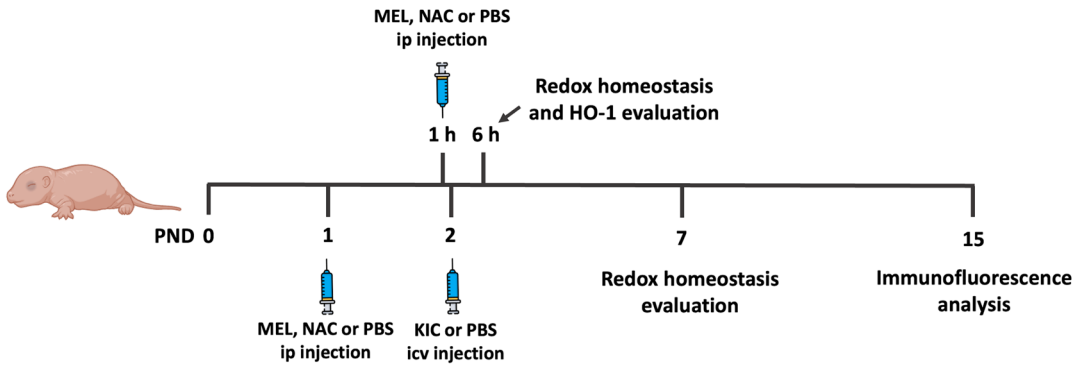

Fig. 1 Schematic representation of the experimental design showing the procedures performed in Wistar rats from postnatal day 1 (PND 1) to postnatal day 15 (PND 15). HO-1, heme oxygenase-1; icv, intracerebroventricular; ip, intraperitoneal; KIC, α-ketoisocaproic acid; MEL, melatonin; NAC, N-acetylcysteine; PND, postnatal day; PBS, phosphate-buffered saline

Nitrate and Nitrite Levels

Reactive nitrogen species (RNS) levels were evaluated by the determination of the nitric oxide derivatives nitrate (NO_3^-) and nitrite (NO_2^-), according to the method described by Navarro-Gonzálvez et al. [37]. Tissue homogenates were deproteinized by a solution of 75 mM $ZnSO_4$, centrifuged, and the supernatant neutralized with a solution of 55 mM NaOH. Then, all nitrates were converted to nitrite by the addition of copper-coated cadmium granules. Next, an aliquot of the samples was treated with the Griess reagent and incubated for 10 min at room temperature in the dark. The absorbance was determined in a Spectramax M5 microplate reader at 505 nm. A standard curve was performed with sodium nitrite (2.5–100 µM). Results were expressed as µmol nitrates and nitrites per milligram protein.

Malondialdehyde (MDA) Levels

MDA levels were determined by measuring thiobarbituric acid reactive substances, according to the method of Yagi [38]. After pre-incubation, tissue homogenates were incubated for 1 h at 100 °C in the presence of 10% trichloroacetic acid (TCA) and 0.67% thiobarbituric acid. The resultant pink color was extracted with butanol and separated by centrifugation. The fluorescence of the organic phase was measured at 515 nm (excitation) and 553 nm (emission). A standard curve was made by using 1,1,3,3-tetramethoxypropane. Results were expressed as nmol MDA per milligram protein.

Carbonyl Content

In order to determine the carbonyl content, tissue homogenates were treated with 2,4-dinitrophenylhydrazine (10 mM) and incubated for 1 h in the dark at room temperature. Proteins were precipitated with 20% TCA, the sediment obtained after centrifugation was washed with a mixture of ethanol:ethyl acetate (1:1, v/v) and resuspended in 6 M guanidine. The carbonyl content was spectrophotometric determined at 365 nm in a Spectramax M5 [39]. Results were expressed as nmol carbonyl content per milligram protein.

Reduced Glutathione (GSH) Levels

Tissue homogenates reacted with o-phthaldialdehyde (1 mg/mL) and were incubated for 15 min at room temperature in the dark. Next, the fluorescence was determined in Spectramax M5 microplates at 350 nm (excitation) and 420 nm (emission) [40]. GSH levels were calculated from a standard curve of GSH (0.001–1 mM) as nmol GSH per milligram protein.

Glutathione Peroxidase (GPx) Activity

GPx activity was determined in tissue homogenates by the method of Wendel [41], using tert-butyl hydroperoxide as substrate. The decrease of NADPH absorbance at 340 nm was monitored in a Spectramax M5. GPx activity was expressed as unit per milligram protein.

Glutathione Reductase (GR) Activity

GR activity was measured in tissue homogenates according to the method described by Carlberg and Mannervik [42], using oxidized glutathione (GSSG) and NADPH as substrates. This enzymatic activity was determined by monitoring the decrease of NADPH absorbance at 340 nm in a Spectramax M5. GR activity was expressed as unit per milligram protein.

Superoxide Dismutase (SOD) Activity

SOD activity was measured in tissue homogenates according to the method of Marklund [43], which is based on the autoxidation of pyrogallol that can be measured by determining the absorbance at 420 nm in a Spectramax M5. A standard curve was made with commercially purified SOD (S8408, Merck) to calculate the SOD activity. The results were expressed as unit per milligram protein.

Western Blotting

For the determination of HO-1 protein immunocontent, animals were euthanized by decapitation; the cerebral cortex was dissected, homogenized, and centrifuged; and the supernatants were prepared for the analyses, as described by Seminotti et al. [33]. The primary antibody anti-HO-1 (1:500, Abcam ab13248) was used and the results expressed as a ratio comparative to β-actin (1:20000, Merck A1978).

Neurochemical Markers

The neurochemical markers were measured by immunofluorescence. A transcardiac perfusion with 0.9% saline containing 0.16% sodium citrate was first carried out in the anesthetized rats and followed by a second perfusion with 4% paraformaldehyde, after which the brain was removed and coronal slices (35 µm) prepared using a Vibratome (VT1000S; Leica, Nussloch, Germany). Three transverse brain slices containing the cerebral cortex and striatum were obtained from each animal and the immunostaining

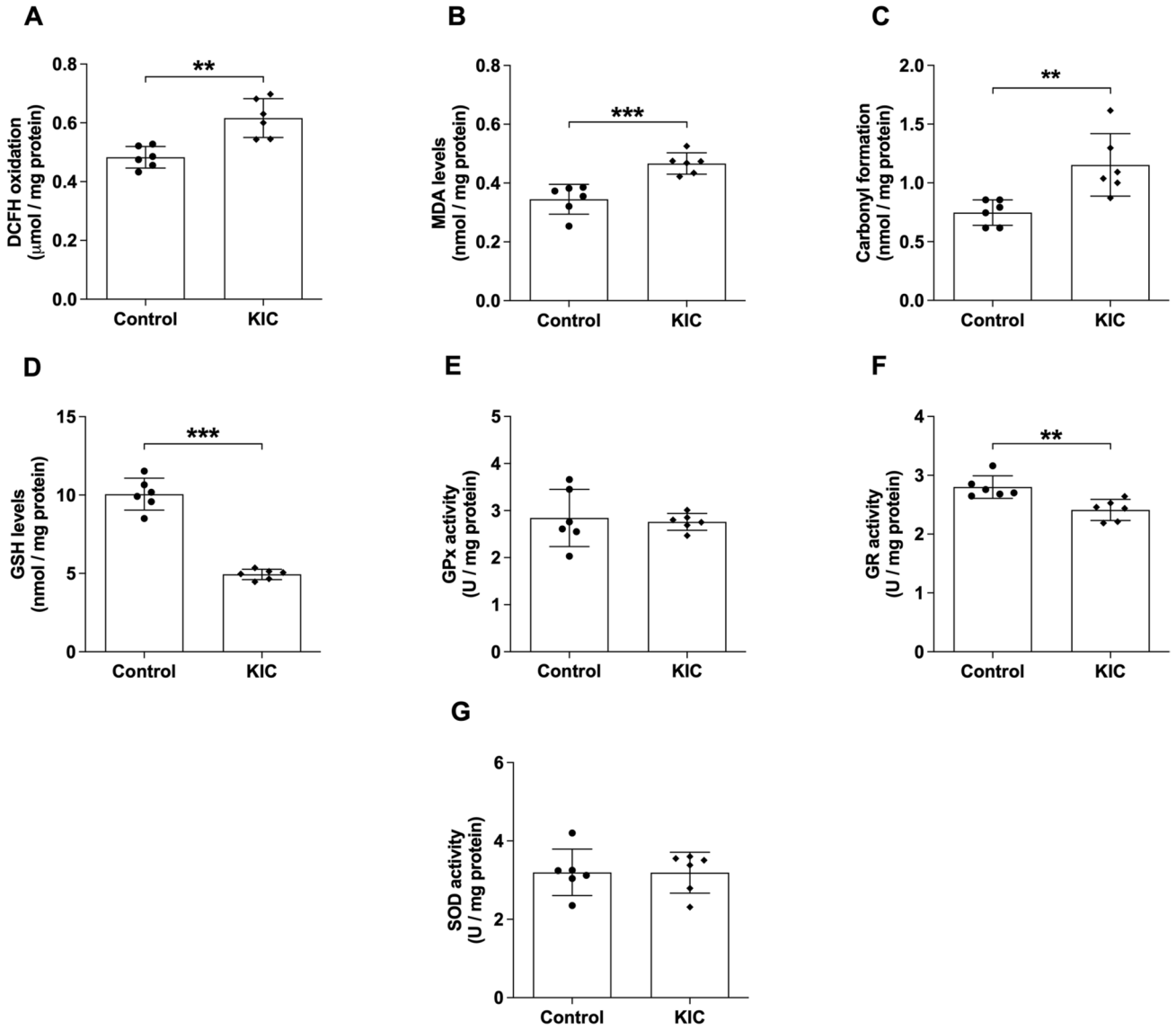

Fig. 2 Effects of an intracerebroventricular (icv) administration of KIC (1 µmol/g) to neonate rats on redox homeostasis in the cerebral cortex 6 hours after injection. 2′,7′-Dichlorofluorescein (DCFH) oxidation (**A**), malondialdehyde (MDA) levels (**B**), carbonyl formation (**C**), reduced glutathione (GSH) levels (**D**), and glutathione peroxidase (GPx) (**E**), glutathione reductase (GR) (**F**), and superoxide dismutase (SOD) (**G**) activities were determined. Values are mean ± standard deviation of six independent experiments (N) expressed as µmol/mg protein, nmol/mg protein or U/mg protein. $^{**}P < 0.01$, $^{***}P < 0.001$ compared to control (Student's *t* test for unpaired samples)

procedures were performed according to Seminotti et al. [33]. An overnight incubation at 4 °C with the following primary antibodies were then performed: mouse anti-neuronal nuclear protein (NeuN) (1:400, Millipore #MAB377), rabbit anti-glial fibrillary acidic protein (GFAP) (1:500, Thermo Fisher # MA5-12,023), mouse anti-myelin basic protein (MBP) (1:500, Merck #AMAb91064), and rabbit anti-2′,3′-cyclic-nucleotide 3′-phosphodiesterase (CNPase) (1:500, Cell Signaling #D83E10). Next, a 90-min incubation at room temperature with a secondary mouse or rabbit antibody was carried out (1:500, Thermo Fisher Scientific). Slices were then assembled with fluoroshield (Merck) and the images were captured by an Olympus FV300 confocal microscope using 488 and 546 nm wavelengths. NeuN-positive cells and the fluorescence intensity of GFAP, MPB, and CNPase were assessed in three randomly chosen fields per slice.

Determination of Protein Concentrations

Protein concentrations were measured by the method of Lowry and collaborators [44] with bovine serum albumin as standard.

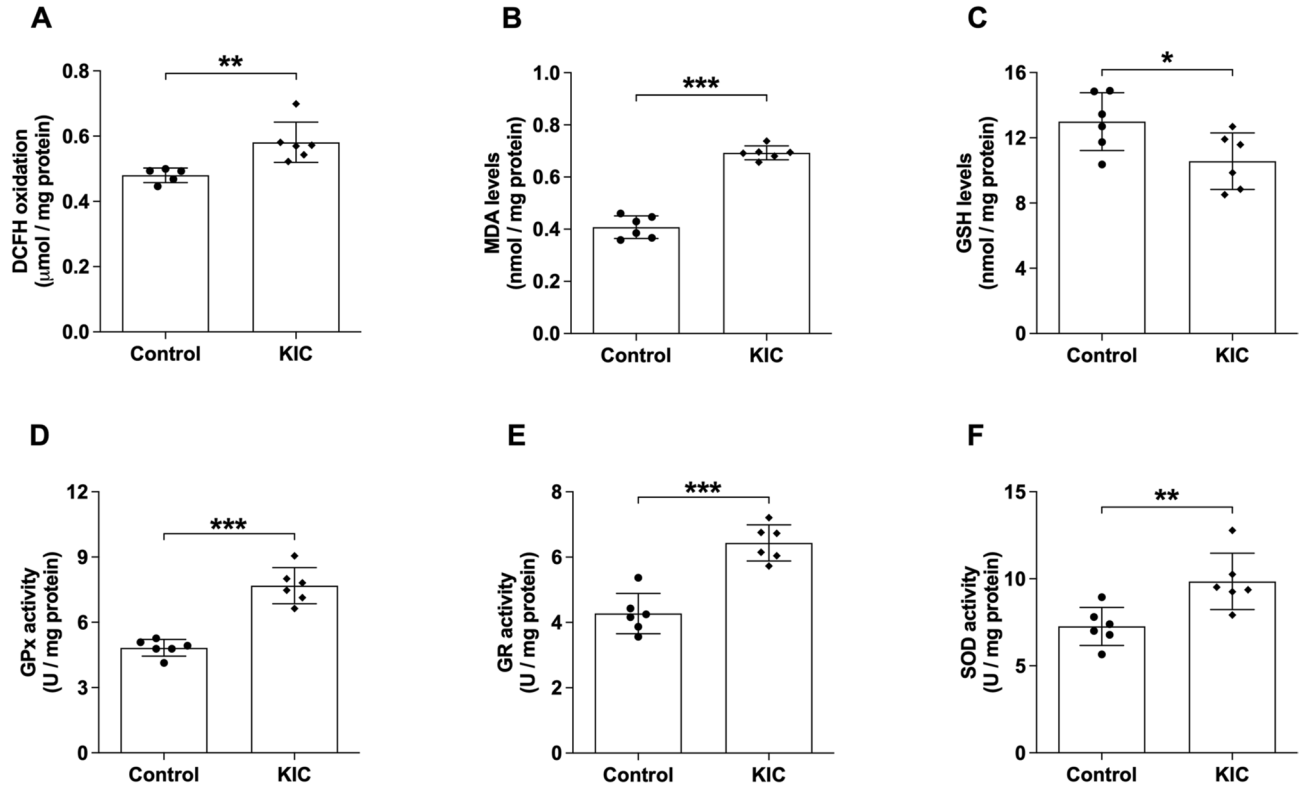

Fig. 3 Effects of an intracerebroventricular (icv) administration of KIC (1 µmol/g) to neonate rats on redox homeostasis in the striatum 6 hours after injection. 2′,7′-Dichlorofluorescein (DCFH) oxidation (**A**), malondialdehyde (MDA) levels (**B**), reduced glutathione (GSH) levels (**C**), and glutathione peroxidase (GPx) (**D**), glutathione reductase (GR) (**E**), and superoxide dismutase (SOD) (**F**) activities were determined. Values are mean ± standard deviation of five to six independent experiments (N) expressed as µmol/mg protein, nmol/mg protein, or U/mg protein. *$P < 0.05$, **$P < 0.01$, ***$P < 0.001$ compared to control (Student's *t* test for unpaired samples)

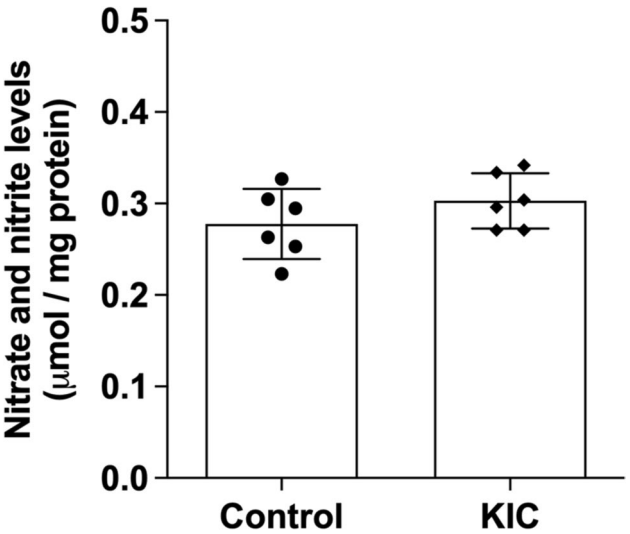

Fig. 4 Effects of an intracerebroventricular (icv) administration of KIC (1 µmol/g) to neonate rats on nitrate and nitrite concentrations in the forebrain 6 h after injection. Values are mean ± standard deviation of six independent experiments (N) expressed as µmol/mg protein. No significant differences were detected (Student's *t* test for unpaired samples)

Statistical Analysis

The normality of data distribution was initially assessed using the Shapiro-Wilk test, which showed a normal distribution pattern. Thus, the statistical analyses were one-way analysis of variance (ANOVA) followed by Tukey's post hoc test when more than two groups were compared, whereas Student's *t* test for unpaired samples was used to compare two groups. Results were expressed as mean ± standard deviation and differences rated significant when $P < 0.05$. All analyses were made in the GraphPad Prism 9.0 software.

Results

Markers of Redox Homeostasis

Cerebral cortex and striatum of neonate rats were assayed to determine a large spectrum of redox homeostasis parameters 6 h after KIC icv injection (1 µmol/g) or at PND 7.

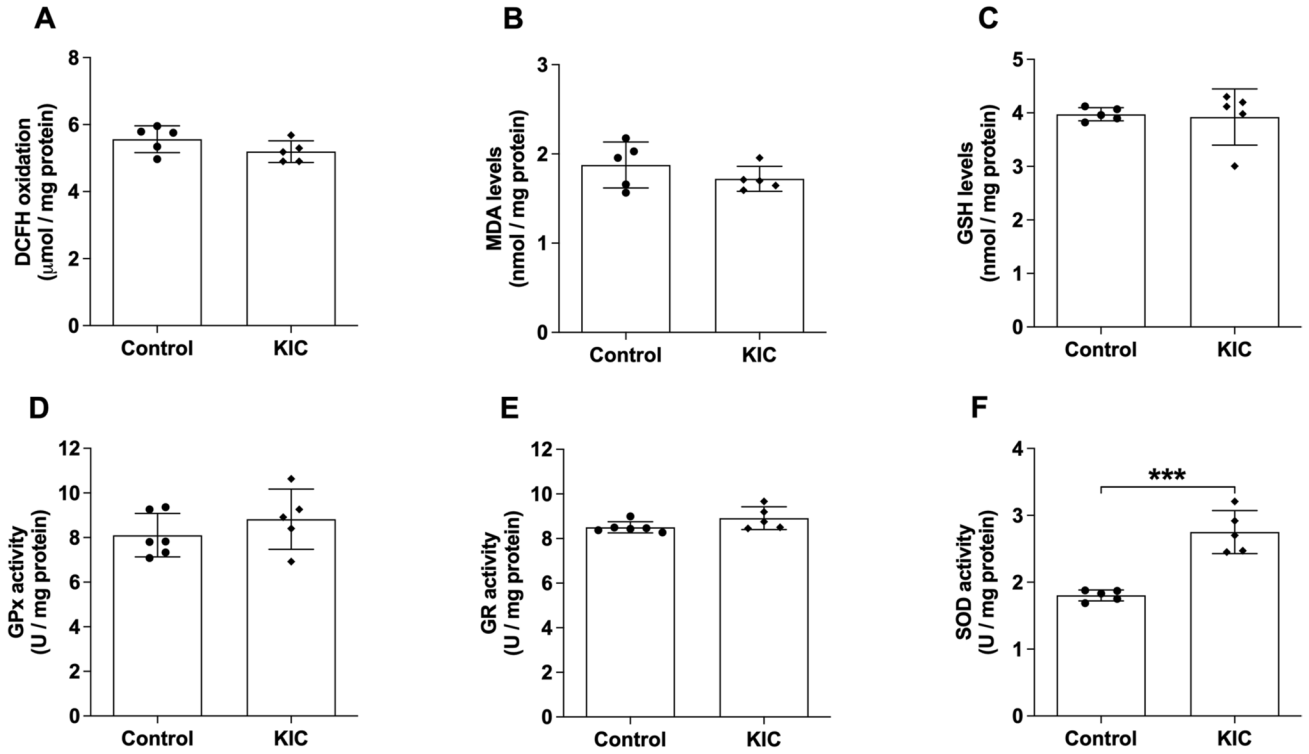

Fig. 5 Effects of an intracerebroventricular (icv) administration of KIC (1 µmol/g) to neonate rats on redox homeostasis in the cerebral cortex at postnatal day (PND) 7. 2′,7′-Dichlorofluorescein (DCFH) oxidation (**A**), malondialdehyde (MDA) levels (**B**), reduced glutathione (GSH) levels (**C**), and glutathione peroxidase (GPx) (**D**), glutathione reductase (GR) (**E**), and superoxide dismutase (SOD) (**F**) activities were evaluated. Values are mean ± standard deviation of five to six independent experiments (N) expressed as µmol/mg protein, nmol/mg protein, and U/mg protein. ***$P < 0.001$ compared to control (Student's *t* test for unpaired samples)

icv Administration of KIC to Neonate Rats Disrupts Brain Redox Homeostasis

We initially observed that icv KIC administration caused significant increases of DCFH oxidation ($t_{(10)} = 4.329$, $P < 0.01$), MDA levels ($t_{(10)} = 4.769$, $P < 0.001$), and carbonyl content ($t_{(10)} = 3.458$, $P < 0.01$), besides a decrease of GSH levels ($t_{(10)} = 11.72$, $P < 0.001$), and GR activity ($t_{(10)} = 3.649$, $P < 0.01$) in the cerebral cortex of the neonate rats 6 h after icv injection. In contrast, SOD and GPx activities were not changed by this treatment (Fig. 2). Furthermore, increased DCFH oxidation ($t_{(9)} = 3.449$, $P < 0.01$) and MDA levels ($t_{(10)} = 13.72$, $P < 0.001$), and decreased GSH concentrations ($t_{(10)} = 2.4$, $P < 0.05$) were observed in the striatum of neonate rats following KIC treatment (Fig. 3). Increased activities of GPx ($t_{(10)} = 7.641$, $P < 0.001$), GR ($t_{(10)} = 6.389$, $P < 0.001$), and SOD ($t_{(10)} = 3.235$, $P < 0.01$) were also found in the striatum 6 h after KIC injection (Fig. 3). Finally, we found that nitrate and nitrite concentrations were not changed in the forebrain of neonate rats 6 h after the administration of the metabolite (Fig. 4). Taken together, these data clearly reveal that a single icv in vivo KIC injection causes short-lived oxidative stress in the brain of neonate rats probably secondary to increased ROS formation.

We also measured the effects of icv KIC injection to the neonate rats on redox homeostasis parameters in cerebral cortex and striatum at PND 7. We observed that KIC only significantly elevated SOD activity ($t_{(8)} = 6.392$, $P < 0.001$) in cerebral cortex, with no alterations of DCFH oxidation, MDA and GSH concentrations, as well as of GPx and GR activities (Fig. 5). Regarding the striatum, we found that all antioxidant enzymes had their activities increased by this treatment (GPx: $t_{(8)} = 9.987$, $P < 0.001$; GR: $t_{(8)} = 2.483$, $P < 0.05$; SOD: $t_{(8)} = 4.249$, $P < 0.01$), without any change in DCFH oxidation, MDA, and GSH levels (Fig. 6).

NAC and MEL Prevent the Alterations Induced by an icv Administration of KIC on Redox Homeostasis in Cerebral Cortex and Striatum of Neonate Rats

Next, we evaluated whether the antioxidants NAC and MEL (intraperitoneal injections 24 and 1 h before KIC administration) could prevent the alterations of the various redox homeostasis parameters caused by KIC administration 6 h after the injection. We found that MEL normalized DCFH

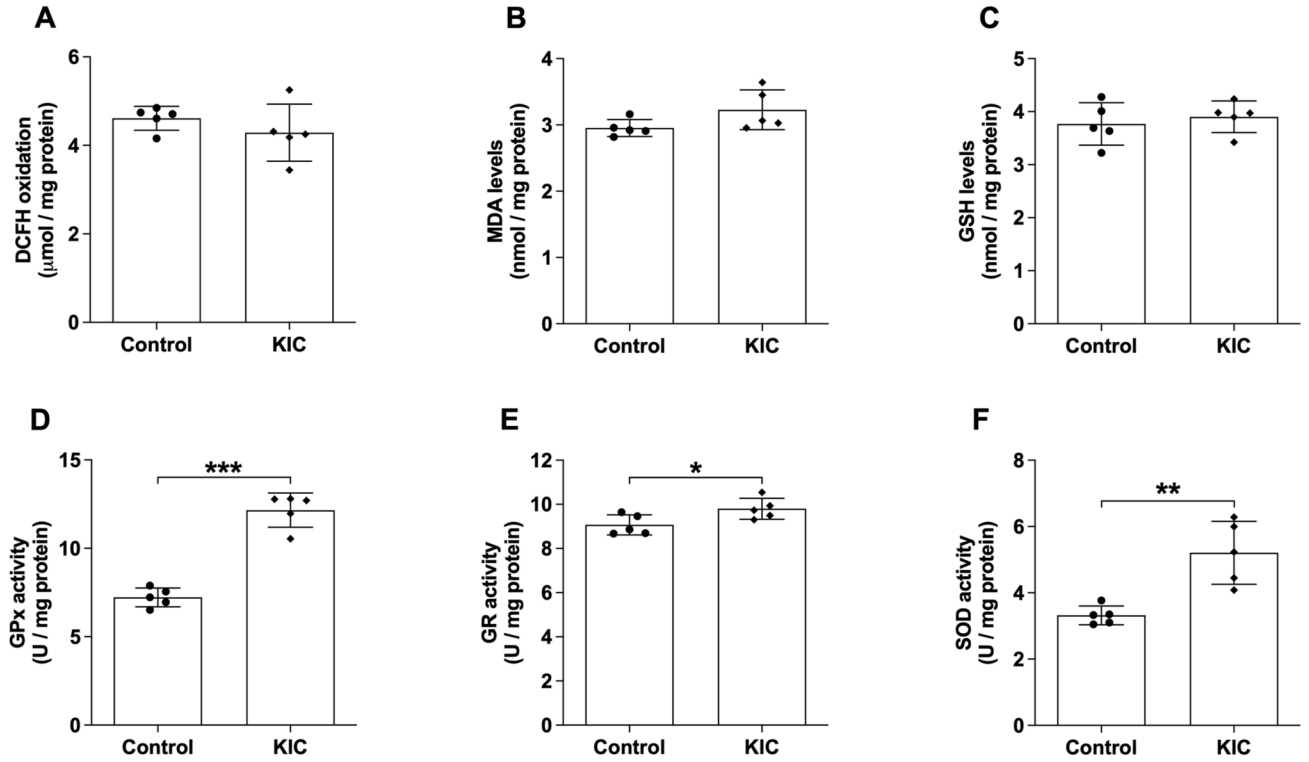

Fig. 6 Effects of an intracerebroventricular (icv) administration of KIC (1 µmol/g) to neonate rats on redox homeostasis in the striatum at postnatal day (PND) 7. 2′,7′-Dichlorofluorescein (DCFH) oxidation (**A**), malondialdehyde (MDA) levels (**B**), reduced glutathione (GSH) levels (**C**), and glutathione peroxidase (GPx) (**D**), glutathione reductase (GR) (**E**), and superoxide dismutase (SOD) (**F**) activities were evaluated. Values are mean ± standard deviation of five independent experiments (N) expressed as µmol/mg protein, nmol/mg protein, and U/mg protein. $^{*}P < 0.05$, $^{**}P < 0.01$, $^{***}P < 0.001$ compared to control (Student's *t* test for unpaired samples)

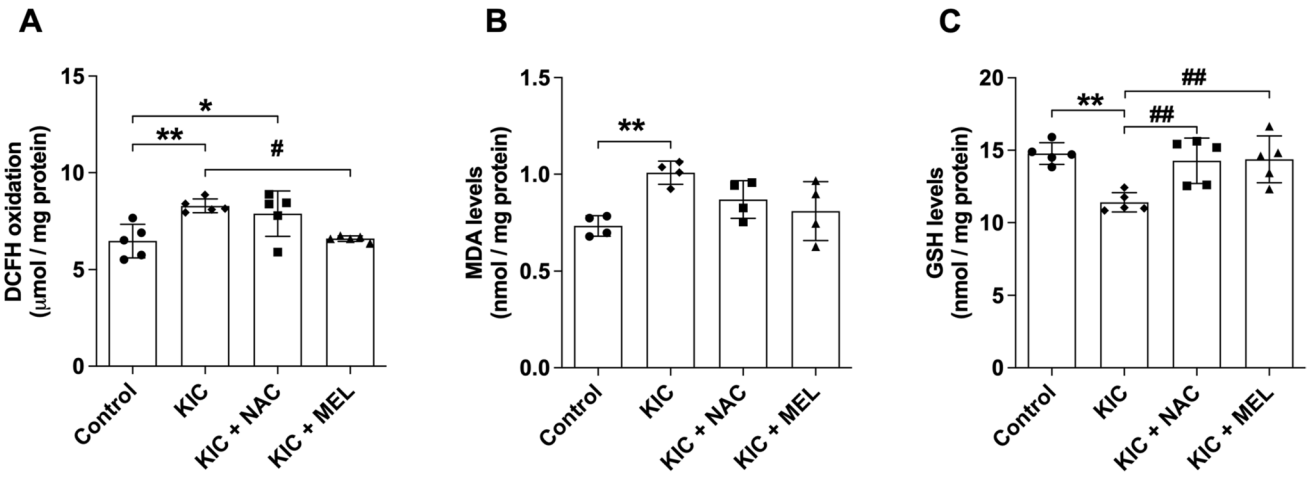

Fig. 7 Effects of the antioxidants N-acetylcysteine (NAC) and melatonin (MEL) on the alterations of redox homeostasis parameters caused by an intracerebroventricular (icv) administration of KIC (1 µmol/g) to neonate rats in the cerebral cortex 6 h after the injection. 2′,7′-Dichlorofluorescein (DCFH) oxidation (**A**), malondialdehyde (MDA) levels (**B**), and reduced glutathione (GSH) levels (**C**) were determined. Animals received two intraperitoneal injections of NAC (300 mg/kg and 400 mg/kg) or MEL (40 mg/kg) 24 and 1 h prior to KIC icv administration. Values are mean ± standard deviation of four to six independent experiments (N) expressed as µmol/mg protein and nmol/mg protein. $^{*}P < 0.05$, $^{**}P < 0.01$ compared to control. $^{\#}P < 0.05$, $^{\#\#}P < 0.01$ compared to KIC (one-way ANOVA, followed by post hoc Tukey's range test)

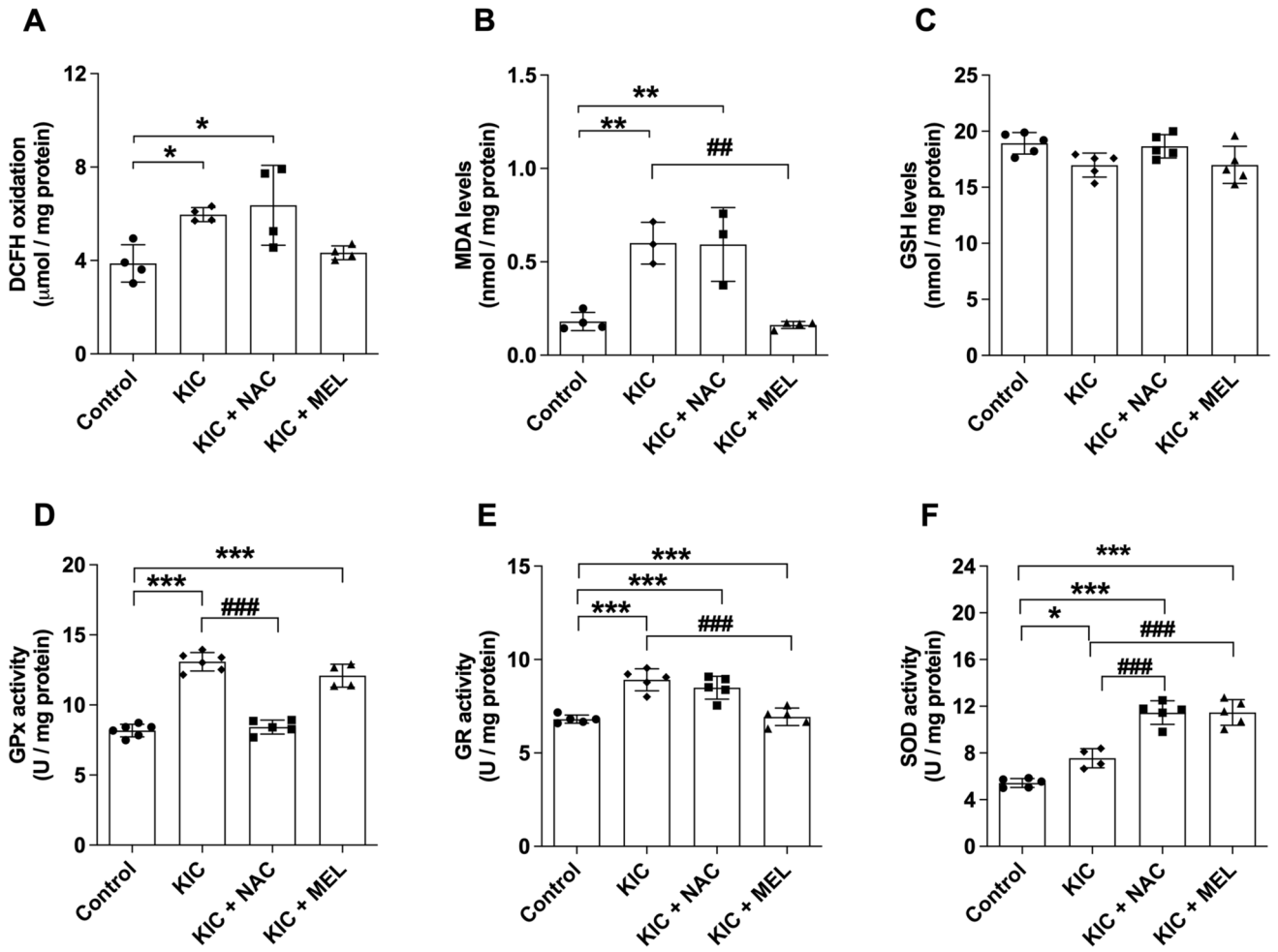

Fig. 8 Effects of the antioxidants N-acetylcysteine (NAC) and melatonin (MEL) on the alterations of redox homeostasis parameters caused by an intracerebroventricular (icv) administration of KIC (1 µmol/g) to neonate rats in the striatum 6 h after the injection. 2′,7′-Dichlorofluorescein (DCFH) oxidation (**A**), malondialdehyde (MDA) levels (**B**), reduced glutathione (GSH) levels (**C**), and the activities of glutathione peroxidase (GPx) (**D**), glutathione reductase (GR) (**E**), and superoxide dismutase (SOD) (**F**) were determined. Animals received two intraperitoneal injections of NAC (300 mg/kg and 400 mg/kg) or MEL (40 mg/kg) 24 and 1 h prior to KIC icv administration. Values are mean ± standard deviation of three to six independent experiments (N) expressed as µmol/mg protein, nmol/mg protein, or U/mg protein. $^{*}P < 0.05$, $^{**}P < 0.01$, $^{***}P < 0.001$ compared to control. $^{\#\#}P < 0.01$, $^{\#\#\#}P < 0.001$ compared to KIC (one-way ANOVA, followed by post hoc Tukey's range test)

oxidation, MDA levels, and GSH concentrations, whereas NAC totally prevented GSH decrease and the increase of MDA levels in the cerebral cortex (Fig. 7) (DCFH: $F_{(3,16)} = 7.359$, $P < 0.01$; MDA: $F_{(3,12)} = 5.555$, $P < 0.05$; GSH: $F_{(3,16)} = 7.861$, $P < 0.01$). Furthermore, MEL fully prevented DCFH oxidation, MDA, and GR activity increase, but did not change KIC-elicited increase of GPx, and exacerbated KIC-induced increase of SOD activity in the striatum. In turn, NAC normalized GPx activity, exacerbated KIC-induced SOD activity increase and did not change KIC-induced alterations on DCFH oxidation, MDA levels and GR activity (Fig. 8) (DCFH: $F_{(3,12)} = 6.313$, $P < 0.01$; MDA: $F_{(3,10)} = 18.67$, $P < 0.001$; GPx: $F_{(3,17)} = 94.67$, $P < 0.001$; GR: $F_{(3,16)} = 23.55$, $P < 0.001$; SOD: $F_{(3,15)} = 57.63$, $P < 0.001$).

icv Administration of KIC to Neonate Rats Induces HO-1 Production in Cerebral Cortex

To find out a possible signaling mechanism involved in the KIC-induced oxidative stress, we measured HO-1 protein levels, an enzyme with cytoprotective effects on oxidative stress by degrading free heme [45], in cerebral cortex of the KIC-treated neonate rats 6 h after injection. Figure 9 shows that the levels of HO-1, which are controlled by the nuclear factor erythroid 2-related factor

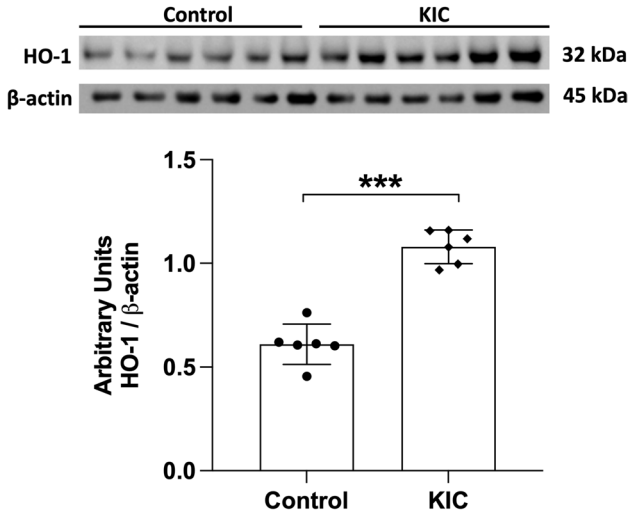

Fig. 9 Effect of an intracerebroventricular (icv) administration of α-ketoisocaproic acid (KIC, 1 µmol/g) to neonate rats on heme oxygenase-1 (HO-1) immunocontent in cerebral cortex 6 h after injection. Values are mean ± standard deviation of three to six independent experiments (N) expressed as arbitrary units. ***$P < 0.001$ compared to control (Student's *t* test for unpaired samples)

2 (Nrf2), were markedly increased after KIC administration ($t_{(10)} = 9.064$, $P < 0.001$).

Neurochemical Markers Measured by Immunofluorescence

We also measured the effects of icv administration of KIC (1 µmol/g) to neonate rats on NeuN, GFAP, MBP, and CNPase immunofluorescence that indicate neuronal number, reactive astrogliosis, and myelination, respectively, in cerebral cortex and striatum at PND 15.

icv Administration of KIC to Neonate Rats Provokes Long-Term Neuronal Loss, Astrocytic Reactivity, and Myelination Impairment at PND 15

Next, we investigated whether an icv administration of KIC to neonate rats could alter the immunofluorescence staining of neuronal (NeuN), astrocytic (GFAP), and myelin (MPB and CNPase) proteins at PND 15. It was found that KIC significantly decreased NeuN (cerebral cortex: $t_{(4)} = 3.301$, $P < 0.05$; striatum: $t_{(4)} = 12.04$, $P < 0.001$) (Fig. 10) and increased GFAP (cerebral cortex: $t_{(5)} = 2.829$, $P < 0.05$; striatum: $t_{(5)} = 2.087$, $P < 0.05$) (Fig. 11) immunofluorescence staining. In addition, MBP (striatum: $t_{(6)} = 2.026$, $P < 0.05$) (Fig. 12) and CNPase (striatum: $t_{(6)} = 2.870$, $P < 0.05$) (Fig. 13) staining were significantly reduced in the striatum of these animals. These results suggest long-term neuronal loss, astrocyte reactivity, and myelination injury in the brain following a single administration of KIC in the neonatal period.

Discussion

MSUD is a severe life-threatening inherited metabolic disease clinically characterized by neurological symptoms that worsen during crises of metabolic decompensation usually triggered by infections and other stressful conditions associated with fasting. These episodes are accompanied by a huge elevation in the levels of the BCKA and BCAA, mainly KIC and leucine, which are thought to be the major neurotoxic metabolites in MSUD [1, 2, 46]. MSUD children that survive the initial episodes of metabolic decompensation during the first weeks of life usually present long-term neurological sequelae, such as cortical atrophy and basal ganglia alterations, whose pathogenesis is still poorly established [8, 47]. In this particular, there is evidence suggesting that oxidative stress and neuroinflammation are associated with MSUD neurodegeneration [27–30, 48–50]. In line with this, various studies found that the metabolites accumulating in this disease disturb redox homeostasis and cause mitochondrial dysfunction in vivo in brain of young and adult rats [11, 13, 18, 22–24, 26]. Furthermore, in vivo icv injection of KIC to 30-day-old rats showed to cause oxidative stress [11], decrease of neurotrophic factors [12], and of respiratory chain complexes activities [13], as well as alterations of pro-inflammatory cytokines levels [14] in various cerebral regions. It is emphasized that most of these experimental works testing the effects of the BCAA and BCKA were carried out using 30-day-old or older rats. Investigating the role of these metabolites on neonatal brain seems therefore justified since MSUD patients manifest with neurological dysfunction in the first days of life.

Thus, the present investigation assessed biochemical markers of oxidative stress and neurochemical landmarks by immunofluorescence staining aiming to determine the number of neurons, astroglial reactivity, and myelination in the cerebral cortex and striatum following an acute cerebral overload of KIC to neonate rats in an effort to clarify the mechanisms responsible for brain injury in MSUD at this age. It is stressed that KIC can easily penetrate into the brain through the monocarboxylate transporter (MCT/SLC16A1) localized in the blood-brain barrier [51–53], being therefore able to accumulate in the central nervous system. We found that KIC caused short-term oxidative stress, as well as long-standing neurochemical alterations indicative of neuronal loss, astrogliosis, and hypo/demyelination in the brain of the treated animals. We also explored whether the antioxidants MEL and NAC could be protective against KIC-induced oxidative stress in these cerebral structures.

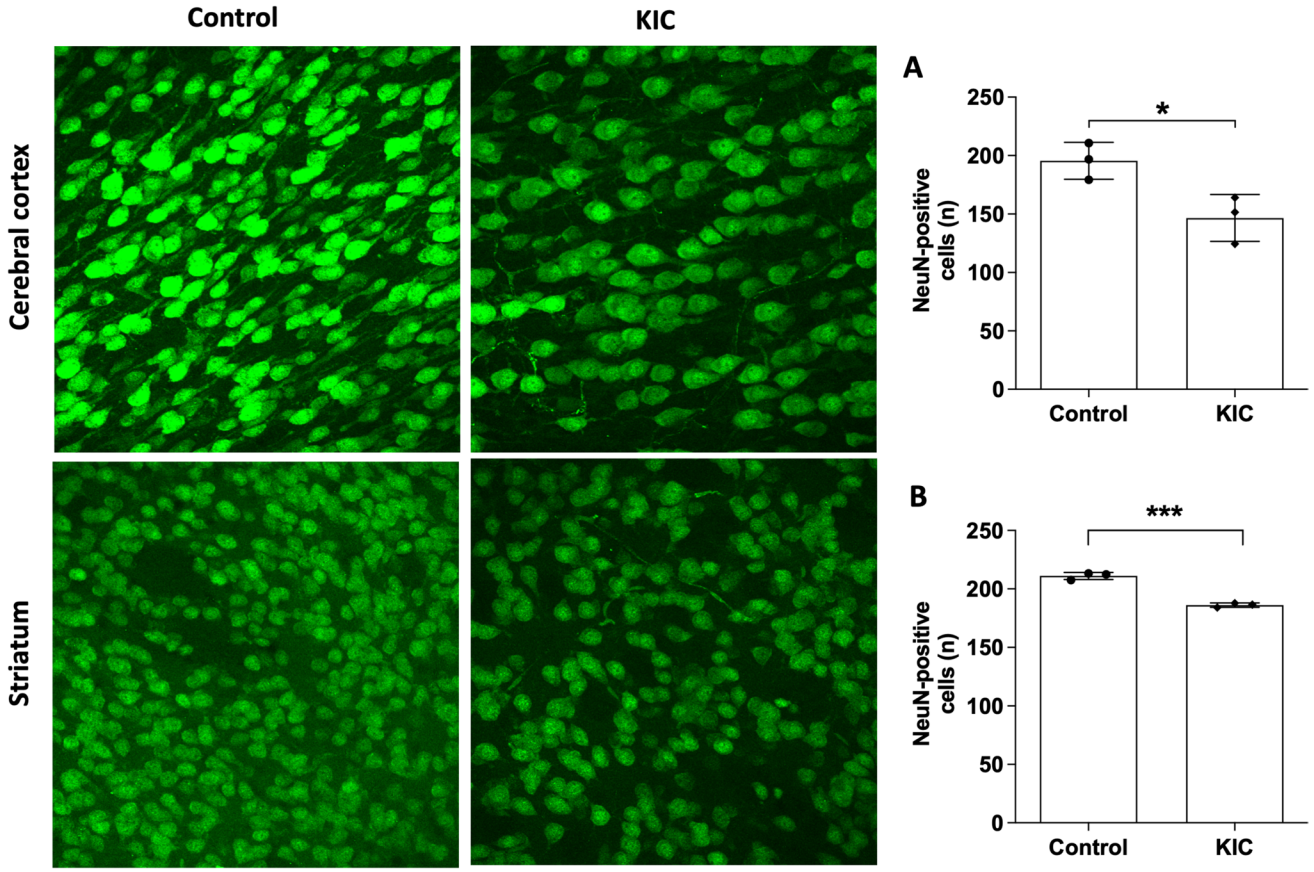

Fig. 10 Effects of an intracerebroventricular (icv) administration of KIC (1 µmol/g) to neonate rats on NeuN immunofluorescence in the cerebral cortex and striatum at postnatal day (PND) 15. Images are representative of three independent experiments (N). Quantitation of NeuN-positive cells was performed on 400× magnification images using the mean of three randomly selected fields of each brain structure per slice. Data were obtained using three slices (containing cerebral cortex and striatum) per rat brain from three animals in each experimental group and are expressed as mean ± standard deviation of NeuN-positive cells. $^{*}P < 0.05$, $^{***}P < 0.001$ compared to control (Student's t test for unpaired samples)

We initially found that KIC increased ROS generation (DCFH oxidation), induced lipid (MDA levels) and protein (carbonyl content) oxidative damage and decreased the GSH levels and GR activity in the cerebral cortex of the neonate rats. Similar findings were obtained in the striatum of these animals, except that all antioxidant enzymes evaluated (GPx, GR, and SOD) had their activities increased. It was also seen that nitrate and nitrite values were not changed by this treatment, ruling out a possible action of RNS in these effects. Noteworthy, since MDA is a lipoperoxidation-derived aldehyde, increases of its levels are indicative of lipid peroxidation, which may lead to severe cell damage, particularly to the brain that is rich in polyunsaturated fatty acids highly vulnerable to oxidation [54, 55]. With respect to the carbonyl groups, they result from the oxidation of amino acid side chain residues, indicating protein oxidation that is potentially harmful to cellular physiology [56, 57].

Regarding the decreased levels of GSH, the primary non-enzymatic antioxidant defense of the central nervous system that is critical to the clearance of free radicals [58], it is feasible that elevated levels of ROS could oxidize GSH, forming GSSG, but this should be confirmed since the oxidized form of GSH was not measured here. We might also suggest that the low capacity to prevent oxidative damage (GSH decrease) caused by KIC in the main structures injured in MSUD, may have contributed to lipid and protein oxidation. In turn, the decreased activity of GR in the cerebral cortex, which is a crucial enzyme to restore GSH concentrations, may also have a role in the diminution of GSH levels. Otherwise, we do not know yet the exact mechanisms for the increased antioxidant enzyme activities in the striatum following KIC injection, but our data showing that this organic acid also increased HO-1 protein content suggest that KIC leads to the upregulation of antioxidant defense genes possibly in an attempt to overcome the redox imbalance generated in this cerebral structure, reflecting therefore a cytoprotective strategy [59, 60].

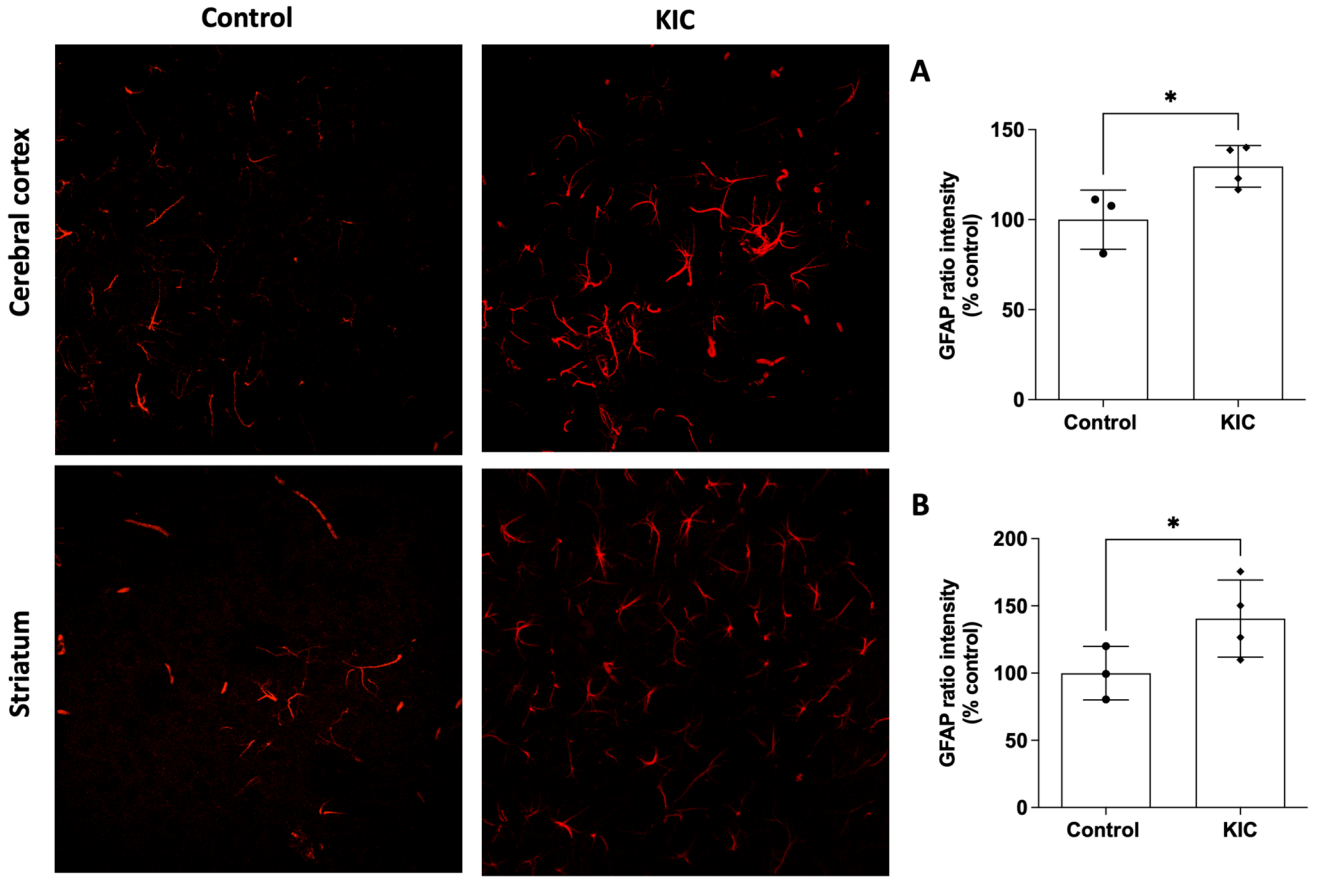

Fig. 11 Effects of an intracerebroventricular (icv) administration of KIC (1 µmol/g) to neonate rats on GFAP immunofluorescence in the cerebral cortex and striatum at postnatal day (PND) 15. Images are representatives of three independent experiments (N). Quantitation of GFAP ratio intensity was performed on 400× magnification images using the mean of three randomly selected fields of each brain structure per slice. Data were obtained using three slices (containing cerebral cortex and striatum) per rat brain from three to four animals in each experimental group and are expressed as mean ± standard deviation of GFAP ratio intensity (% of control). *$P < 0.05$ compared to control (Student's *t* test for unpaired samples)

With respect to SOD, since this enzyme converts the superoxide radical to hydrogen peroxide mainly to preserve GSH [61, 62], it is possible that SOD increased activity could result from its transcriptional overproduction to combat the increase in the anion superoxide radical [63]. The same reasoning could explain GPx activity augment in the striatum, to counterattack hydrogen peroxide species.

Since oxidative stress represents an unbalance between reactive species generation and antioxidant defenses [63], our present findings indicate that KIC induces oxidative stress in the brain of neonate rats, which to our mind was not yet described at this early development stage.

Our results also revealed that pre-treatment of neonate rats with the antioxidants NAC and MEL before KIC injection prevented or attenuated most of the altered biochemical markers of redox homeostasis. Therefore, we presume that particularly NAC, which is used in other pathologies to restore cell redox homeostasis [64–66], could serve as an adjuvant therapy to avoid, or ameliorate acute or chronic oxidative damage to critical cell macromolecules in MSUD.

In this regard, NAC is an effective antioxidant, neutralizing ROS and RNS [67]. This compound has a direct effect due to its free thiol group and it is an essential substrate for the enzyme γ-glutamylcysteine synthetase in the synthesis of GSH [68]. NAC has also anti-inflammatory properties by suppressing the nuclear factor κ B (NF-κB), diminishing the production of tumor necrosis factor-α, interleukin-1, and interleukin-6 (pro-inflammatory cytokines) [69].

MEL, a neurohormone secreted by the pineal gland, acts primarily on circadian rhythms [70], but has been shown to have neuroprotective effects [71, 72] mainly attributed to its antioxidant activity and improvement of mitochondrial function [70, 73–80]. In this context, MEL was demonstrated to mitigate oxidative stress induction by regulating the Nrf2 signaling pathway [81–83], which is mainly responsible for modulating the expression of many antioxidant genes [84].

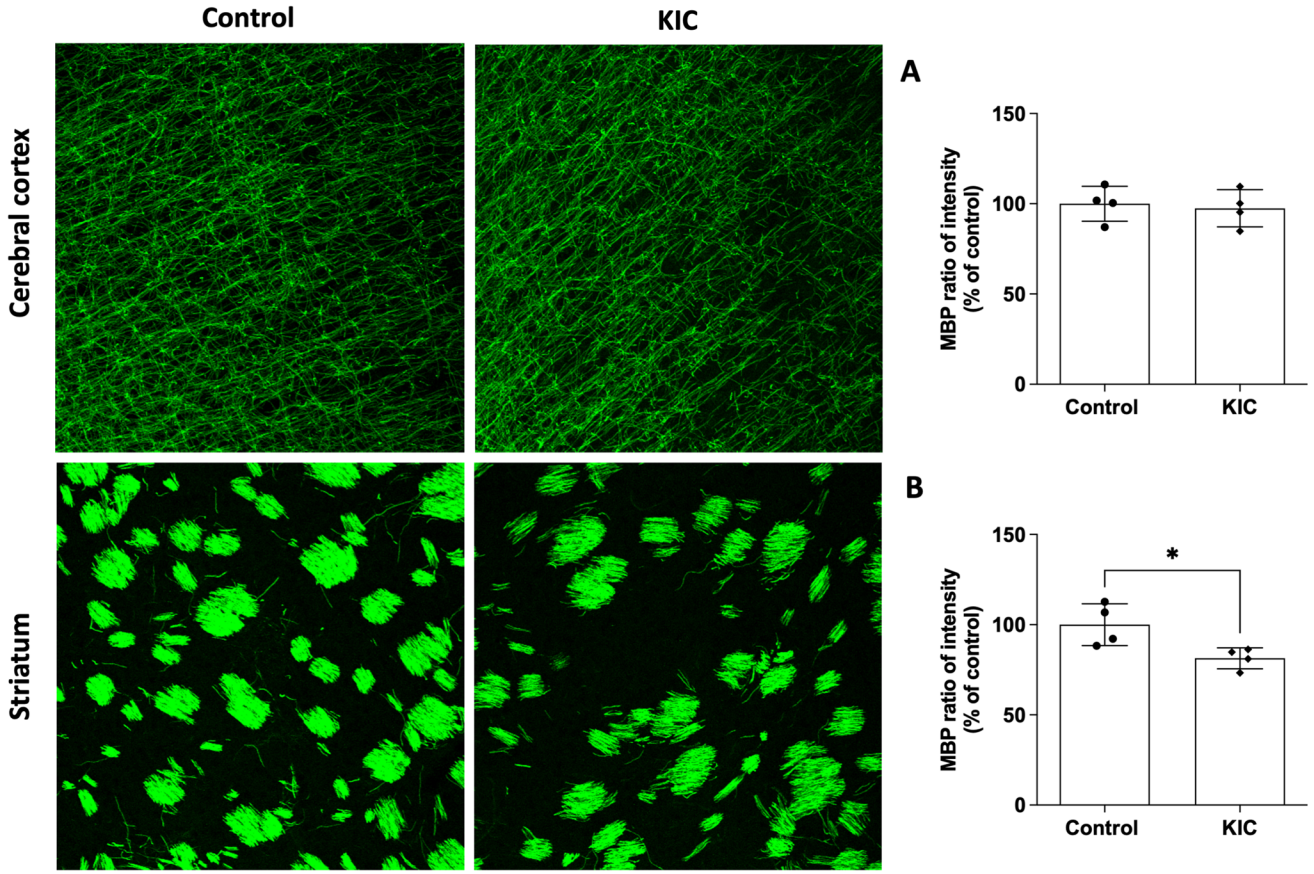

Fig. 12 Effects of an intracerebroventricular (icv) administration of KIC (1 µmol/g) to neonate rats on MBP immunofluorescence in the cerebral cortex (**A**) and striatum (**B**) at postnatal day (PND) 15. Images are representatives of four independent experiments (N). Quantitation of MBP ratio intensity was performed on 200× magnification images using the mean of three randomly selected fields of each brain structure per slice. Data were obtained using three slices (containing cerebral cortex and striatum) per rat brain from four animals in each experimental group and are expressed as mean ± standard deviation of MBP ratio intensity (% of control). *$P < 0.05$ compared to control (Student's *t* test for unpaired samples)

Another interesting observation of this work was that oxidative stress induction following KIC injection at neonatal period was much less evident at PND 7, implying a short-lived effect of this metabolite on brain redox status.

The present data obtained very early during rat development, at an age where severe neurological symptoms appear in humans, are in agreement with previous results that reported increased MDA levels, protein carbonylation, DCFH oxidation, DNA oxidative damage, and SOD activity induced by KIC icv administration in the brain of young rats [11, 13], as well as with in vitro studies demonstrating that KIC disturbs brain redox homeostasis in young rats [15], C6 astroglial cells [16], human leukocytes [85, 86], and hippocampal neuronal cells [13]. Oxidative damage to lipids and proteins has been also shown in plasma of MSUD patients [27–30], corroborating with the in vivo and in vitro animal studies.

We also evaluated whether the injection of KIC to neonate rats could provoke neuronal damage, astrocyte reactivity, and myelination injury in striatum and cerebral cortex at PND 15 since there is no report on whether an acute intracerebral KIC overload during this period of life could cause histopathological alterations along development.

KIC administration led to a long-standing (PND 15) neuronal damage or/and loss (decreased NeuN positive cells) and astroglial reactivity (elevation of the astrocytic marker GFAP) in the cerebral cortex and striatum, whereas significant decreases of the immunoreactivity of the myelin proteins MBP and CNPase, indicating myelination injury, were found in the striatum.

It is emphasized that a moderate activation of astrocytes usually represents a mechanism of protection to surrounding neurons, whereas exacerbated glial reactivity may be deleterious to neurons, as evidenced in various neurodegenerative pathologies [87–89]. Noteworthy, GFAP, which is the main protein constituting astrocyte intermediate filaments, has been considered a classic marker of reactive astrocytes [90, 91]. In this scenario, the present investigation also showed a

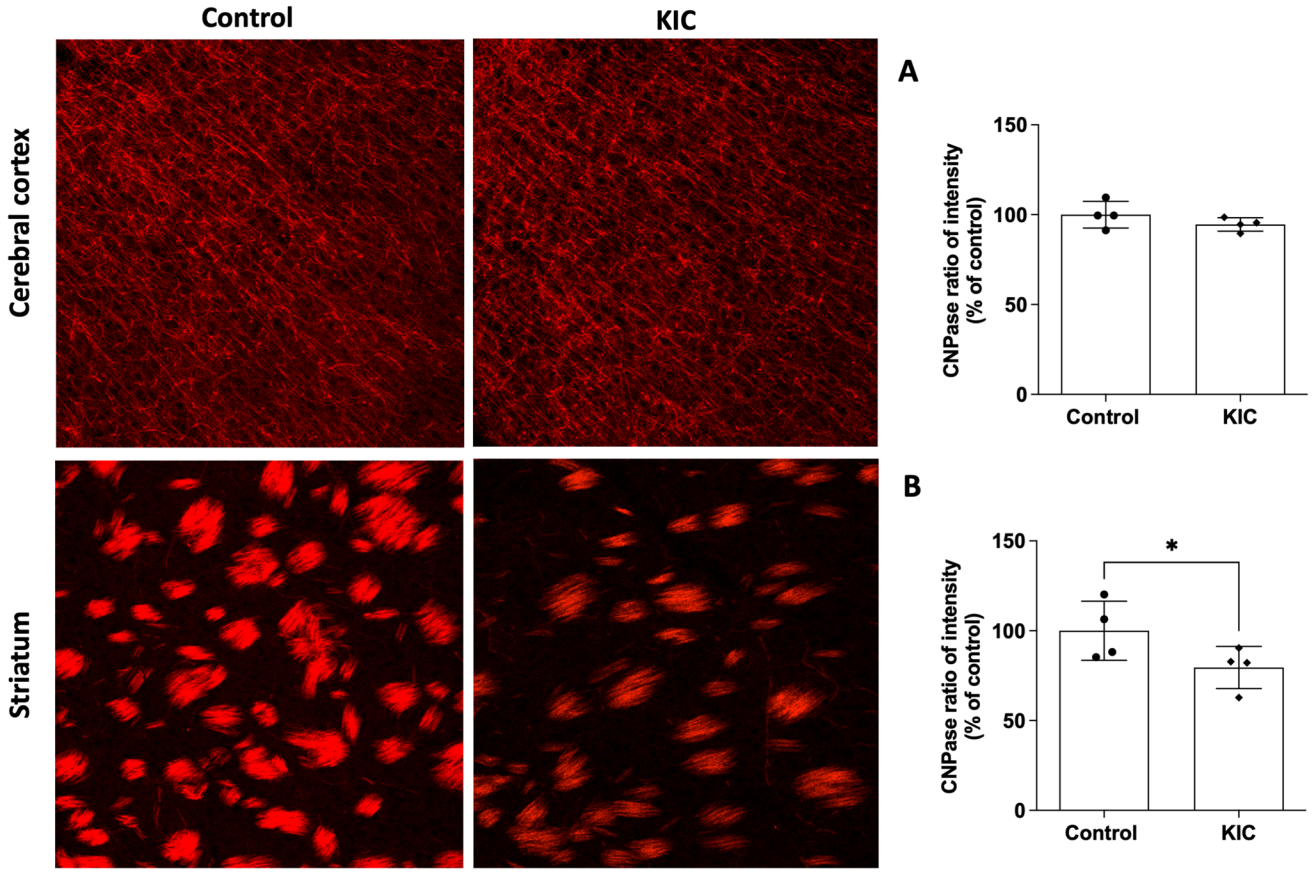

Fig. 13 Effects of an intracerebroventricular (icv) administration of KIC (1 μmol/g) to neonate rats on CNPase immunofluorescence in the cerebral cortex (**A**) and striatum (**B**) at postnatal day (PND) 15. Images are representatives of four independent experiments (N). Quantitation of CNPase ratio intensity was performed on 200× magnification images using the mean of three randomly selected fields of each brain structure per slice. Data were obtained using three slices (containing cerebral cortex and striatum) per rat brain from four animals in each experimental group and are expressed as mean ± standard deviation of CNPase ratio intensity (% of control). $^{*}P < 0.05$ compared to control (Student's *t* test for unpaired samples)

decrease of NeuN immunoreactivity in cerebral cortex and striatum, suggesting neuronal damage associated with glial reactivity in these cerebral structures that are mostly injured in MSUD.

In what concerns to myelination, we found a significant decrease of the content of sensitive protein markers of the myelination status in the striatum. A significant decrease in MBP immunoreactivity was observed in the striatum at PND 15, indicating myelin vulnerability secondary to neonatal intracerebral accumulation of KIC. Of note, the MBP is a sensitive marker of oligodendrocyte function and myelination status once it maintains myelin stability and integrity [92, 93]. In addition, MBP is involved in the maintenance of calcium and cell homeostasis [93]. The immunoreactivity of the CNPase protein, which is important in the regulation of oligodendrocyte process outgrowth [94, 95], was also significantly reduced in the striatum of these animals at PND 15, further indicating myelin injury in the rats neonatally injected with KIC. No significant effect of this treatment towards myelination was observed in the cerebral cortex, indicating that striatum is more vulnerable to myelin injury caused by an acute overload of KIC during the neonatal period that possibly mimics a metabolic episode of decompensation in MSUD affected neonates.

The present neurochemical findings corroborate with previous post-mortem studies carried out in MSUD patients showing defective myelination in various brain regions, including subcortical areas and basal ganglia [96, 97], as well as decrease of oligodendrocyte number in brain white matter [97–99], neuronal abnormalities in the cerebral cortex, and astrogliosis in the hippocampus and basal ganglia [100].

It should be also emphasized that the development and formation of a normal adult brain may be affected by injuries in the early postnatal period that lead to future neurologic symptoms and brain abnormalities. In this particular, it is interesting to note that all KIC-injected animals manifested with seizures immediately after its administration and

recovered after approximately 5 min, in contrast to the PBS-injected rats (controls) that had no seizures at all. These observations revealed that our model of MSUD was toxic to the animals. Based on the data of the present investigation, we postulate that intracerebral toxic levels of KIC at the neonatal period may imbalance cellular redox status, disturbing cellular functions, and ultimately leading to neuronal loss, astrocyte reactivity, and myelination impairment.

We cannot, however, rule out that other pathomechanisms of brain damage are caused by increased concentrations of KIC or of the other metabolites accumulated in MSUD, including mitochondrial dysfunction and increased inflammatory response [46], that may also play an important role in MSUD neuropathology. In this context, we highlight that oxidative stress and neuroinflammation are inter-connected pathogenic processes [101], so that it is feasible that increased pro-inflammatory cytokines in the neural cells might also contribute to the deleterious effects caused by KIC. Indeed, elevation of these inflammatory biomarkers was demonstrated in MSUD patients [48, 50] and in animal models of this disease [102, 103]. However, further studies are required to corroborate this hypothesis.

In conclusion, the findings obtained in this study indicate that KIC-induced oxidative stress early during development may represent a central deleterious mechanism involved in neurological injury in MSUD and that antioxidants may represent a potential new therapeutic strategy for patients affected by this disease. We emphasize that the main purpose of our experimental model using a single icv administration of KIC was to mimic the acute episodes of metabolic decompensation that take place during stressful situations in MSUD patients and are accompanied by high elevation of the brain levels of the accumulating metabolites, particularly KIC. It is also of note that in the affected patients KIC produced peripherally may enter the brain from the systemic circulation, being transported through the blood-brain barrier where it accumulates [53]. Furthermore, this organic acid can be also produced from leucine and accumulate inside the brain cells of MSUD patients, because of the deficient activity of the BCKDH complex in this tissue [53].

Acknowledgements We thank the Centro de Microscopia e Microanálise (UFRGS, RS, Brazil) for the support with the immunofluorescence analysis.

Author Contribution A.B.Z. performed experiments, prepared the figures, and analyzed the data; R.T.R. and C.V.P. performed experiments and analyzed the data; S.A.C., T.Q.T., and E.T.C. provided assistance to the experiments; G.L. analyzed the data and corrected the manuscript text; M.W. and A.U.A. planned the experiments, analyzed the data, and wrote the main manuscript text. All authors read and approved the final manuscript.

Funding This work was supported by grants from Conselho Nacional de Desenvolvimento Científico e Tecnológico (CNPq, 402440/2021-8), Fundação de Amparo à Pesquisa do Estado do Rio Grande do Sul (FAPERGS, 19/2551-0001662-0), Instituto Nacional de Ciência e Tecnologia – Excitotoxicidade e Neuroproteção (INCT-EN, 465671/2014–4), and Instituto Nacional de Ciência e Tecnologia – Saúde Cerebral (INCT-SC, 406020/2022-1).

Data Availability The datasets generated during and/or analyzed during the current study are available from the corresponding author on reasonable request.

Declarations

Ethics Approval The experimental procedures of this study were approved by the Ethical Committee of UFRGS (nº 42875) and performed according to the Guide for the Care and Use of Laboratory Animals (Eighth edition, 2011).

Consent to Participate Not applicable.

Consent to Publish Not applicable.

Competing Interests The authors declare no competing interests.

References

1. Chuang DT, Shih VE, Wynn RM (2019) Maple syrup urine disease (branched-chain ketoaciduria). In: Valle DL, Antonarakis S, Ballabio A, Beaudet AL, Mitchell GA (eds) The online metabolic and molecular bases of inherited disease. McGraw-Hill, New York City (NY), pp. 1–74. https://doi.org/10.1036/Ommbid.400
2. Strauss KA, Carson VJ, Soltys K et al (2020) Branched-chain α-ketoacid dehydrogenase deficiency (maple syrup urine disease): treatment, biomarkers, and outcomes. Mol Genet Metab 129:193–206. https://doi.org/10.1016/J.YMGME.2020.01.006
3. Chen T, Lu D, Xu F et al (2023) Newborn screening of maple syrup urine disease and the effect of early diagnosis. Clin Chim Acta 548:117483. https://doi.org/10.1016/J.CCA.2023.117483
4. Li L, Mao X, Yang N et al (2023) Identification of gene mutations in six Chinese patients with maple syrup urine disease. Front Genet 14:1132364. https://doi.org/10.3389/FGENE.2023.1132364
5. Allahwala A, Ahmed S, Afroze B (2021) Maple syrup urine disease: magnetic resonance imaging findings in three patients. J Pak Med Assoc 71:1–11. https://doi.org/10.47391/JPMA.1341
6. Cheng A, Han L, Feng Y et al (2017) MRI and clinical features of maple syrup urine disease: preliminary results in 10 cases. Diagn Interv Radiol 23:398–402. https://doi.org/10.5152/DIR.2017.16466
7. Kathait AS, Puac P, Castillo M (2018) Imaging findings in maple syrup urine disease: a case report. J Pediatr Neurosci 13:103–105. https://doi.org/10.4103/JPN.JPN_38_17
8. Muelly ER, Moore GJ, Bunce SC et al (2013) Biochemical correlates of neuropsychiatric illness in maple syrup urine disease. J Clin Invest 123:1809–1820. https://doi.org/10.1172/JCI67217
9. Schönberger S, Schweiger B, Schwahn B et al (2004) Dysmyelination in the brain of adolescents and young adults with maple syrup urine disease. Mol Genet Metab 82:69–75. https://doi.org/10.1016/J.YMGME.2004.01.016
10. Vasques VDC, De Boer MA, Diligenti F et al (2004) Intrahippocampal administration of the α-keto acids accumulating in maple syrup urine disease provokes learning deficits in rats. Pharmacol Biochem Behav 77:183–190. https://doi.org/10.1016/j.pbb.2003.10.013

11. Taschetto L, Scaini G, Zapelini HG et al (2017) Acute and long-term effects of intracerebroventricular administration of α-ketoisocaproic acid on oxidative stress parameters and cognitive and noncognitive behaviors. Metab Brain Dis 32:1507–1518. https://doi.org/10.1007/S11011-017-0035-Z
12. Wisniewski MSW, Carvalho-Silva M, Gomes LM et al (2016) Intracerebroventricular administration of α-ketoisocaproic acid decreases brain-derived neurotrophic factor and nerve growth factor levels in brain of young rats. Metab Brain Dis 31:377–383. https://doi.org/10.1007/S11011-015-9768-8
13. Farias HR, Gabriel JR, Cecconi ML et al (2021) The metabolic effect of α-ketoisocaproic acid: in vivo and in vitro studies. Metab Brain Dis 36:185–192. https://doi.org/10.1007/S11011-020-00626-Y
14. Rabelo F, Lemos ID, Dal Toé CP et al (2023) Acute effects of intracerebroventricular administration of α-ketoisocaproic acid in young rats on inflammatory parameters. Metab Brain Dis 38:1573–1579. https://doi.org/10.1007/S11011-023-01193-8
15. Bridi R, Braun CA, Zorzi GK et al (2005) α-Keto acids accumulating in maple syrup urine disease stimulate lipid peroxidation and reduce antioxidant defences in cerebral cortex from young rats. Metab Brain Dis 20:155–167. https://doi.org/10.1007/s11011-005-4152-8
16. Funchal C, Latini A, Jacques-Silva MC et al (2006) Morphological alterations and induction of oxidative stress in glial cells caused by the branched-chain α-keto acids accumulating in maple syrup urine disease. Neurochem Int 49:640–650. https://doi.org/10.1016/J.NEUINT.2006.05.007
17. Patel MS, Auerbach VH, Grover WD, Wilbur DO (1973) Effect of the branched-chain α-keto acids on pyruvate metabolism by homogenates of human brain. J Neurochem 20:1793–1796. https://doi.org/10.1111/J.1471-4159.1973.TB00298.X
18. Ribeiro CA, Sgaravatti ÂM, Rosa RB et al (2008) Inhibition of brain energy metabolism by the branched-chain amino acids accumulating in maple syrup urine disease. Neurochem Res 33:114–124. https://doi.org/10.1007/S11064-007-9423-9
19. Amaral AU, Leipnitz G, Fernandes CG et al (2010) α-Ketoisocaproic acid and leucine provoke mitochondrial bioenergetic dysfunction in rat brain. Brain Res 1324:75–84. https://doi.org/10.1016/J.BRAINRES.2010.02.018
20. Sgaravatti AM, Rosa RB, Schuck PF et al (2003) Inhibition of brain energy metabolism by the α-keto acids accumulating in maple syrup urine disease. Biochim Biophys Acta 1639:232–238. https://doi.org/10.1016/J.BBADIS.2003.09.010
21. Bridi R, Araldi J, Sgarbi MB et al (2003) Induction of oxidative stress in rat brain by the metabolites accumulating in maple syrup urine disease. Int J Dev Neurosci 21:327–332. https://doi.org/10.1016/S0736-5748(03)00074-1
22. Mescka C, Moraes T, Rosa A et al (2011) In vivo neuroprotective effect of L-carnitine against oxidative stress in maple syrup urine disease. Metab Brain Dis 26:21–28. https://doi.org/10.1007/S11011-011-9238-X
23. Mescka CP, Rosa AP, Schirmbeck G et al (2016) L-Carnitine prevents oxidative stress in the brains of rats subjected to a chemically induced chronic model of MSUD. Mol Neurobiol 53:6007–6017. https://doi.org/10.1007/S12035-015-9500-Z
24. Scaini G, Jeremias IC, Morais MOS et al (2012) DNA damage in an animal model of maple syrup urine disease. Mol Genet Metab 106:169–174. https://doi.org/10.1016/J.YMGME.2012.04.009
25. Pilla C, De Oliveira Cardozo RF, Dutra-Filho CS et al (2003) Effect of leucine administration on creatine kinase activity in rat brain. Metab Brain Dis 18:17–25. https://doi.org/10.1023/A:1021974517837
26. Pilla C, De Oliveira Cardozo RF, Dutra-Filho CS et al (2003) Creatine kinase activity from rat brain is inhibited by branched-chain amino acids in vitro. Neurochem Res 28:675–679. https://doi.org/10.1023/A:1022876130038
27. Barschak AG, Sitta A, Deon M et al (2006) Evidence that oxidative stress is increased in plasma from patients with maple syrup urine disease. Metab Brain Dis 21:279–286. https://doi.org/10.1007/S11011-006-9030-5
28. Guerreiro G, Mescka CP, Sitta A et al (2015) Urinary biomarkers of oxidative damage in maple syrup urine disease: the L-carnitine role. Int J Dev Neurosci 42:10–14. https://doi.org/10.1016/J.IJDEVNEU.2015.02.003
29. Mescka CP, Wayhs CAY, Vanzin CS et al (2013) Protein and lipid damage in maple syrup urine disease patients: L-carnitine effect. Int J Dev Neurosci 31:21–24. https://doi.org/10.1016/J.IJDEVNEU.2012.10.109
30. Mc Guire PJ, Parikh A, Diaz GA (2009) Profiling of oxidative stress in patients with inborn errors of metabolism. Mol Genet Metab 98:173–180. https://doi.org/10.1016/J.YMGME.2009.06.007
31. Olivera-Bravo S, Fernández A, Sarlabós MN et al (2011) Neonatal astrocyte damage is sufficient to trigger progressive striatal degeneration in a rat model of glutaric acidemia-I. PLoS One 6:e20831. https://doi.org/10.1371/JOURNAL.PONE.0020831
32. Ribeiro RT, Seminotti B, Zanatta Â et al (2021) Neuronal death, glial reactivity, microglia activation, oxidative stress and bioenergetics impairment caused by intracerebroventricular administration of D-2-hydroxyglutaric acid to neonatal rats. Neuroscience 471:115–132. https://doi.org/10.1016/J.NEUROSCIENCE.2021.07.024
33. Seminotti B, Zanatta Â, Ribeiro RT et al (2019) Disruption of brain redox homeostasis, microglia activation and neuronal damage induced by intracerebroventricular administration of s-adenosylmethionine to developing rats. Mol Neurobiol 56:2760–2773. https://doi.org/10.1007/S12035-018-1275-6
34. Moura AP, Parmeggiani B, Grings M et al (2016) Intracerebral glycine administration impairs energy and redox homeostasis and induces glial reactivity in cerebral cortex of newborn rats. Mol Neurobiol 53:5864–5875. https://doi.org/10.1007/S12035-015-9493-7
35. Ribeiro RT, Zanatta Â, Amaral AU et al (2018) Experimental evidence that in vivo intracerebral administration of L-2-hydroxyglutaric acid to neonatal rats provokes disruption of redox status and histopathological abnormalities in the brain. Neurotox Res 33:681–692. https://doi.org/10.1007/S12640-018-9874-6
36. LeBel CP, Ischiropoulos H, Bondy SC (1992) Evaluation of the probe 2',7'-dichlorofluorescin as an indicator of reactive oxygen species formation and oxidative stress. Chem Res Toxicol 5:227–231. https://doi.org/10.1021/TX00026A012
37. Navarro-Gonzálvez JA, García-Benayas C, Arenas J (1998) Semiautomated measurement of nitrate in biological fluids. Clin Chem 44:679–681. https://doi.org/10.1093/CLINCHEM/44.3.679
38. Yagi K (1998) Simple procedure for specific assay of lipid hydroperoxides in serum or plasma. Methods Mol Biol 108:107–110. https://doi.org/10.1385/0-89603-472-0:107
39. Reznick AZ, Packer L (1994) Oxidative damage to proteins: spectrophotometric method for carbonyl assay. Methods Enzymol 233:357–363. https://doi.org/10.1016/S0076-6879(94)33041-7
40. Browne RW, Armstrong D (1998) Reduced glutathione and glutathione disulfide. Methods Mol Biol 108:347–352. https://doi.org/10.1385/0-89603-472-0:347
41. Wendel A (1981) Glutathione peroxidase. Methods Enzymol 77:325–333. https://doi.org/10.1016/S0076-6879(81)77046-0

42. Carlberg I, Mannervik B (1985) [59] Glutathione reductase. Methods Enzymol 113:484–490. https://doi.org/10.1016/S0076-6879(85)13062-4
43. Marklund SL (1985) Product of extracellular-superoxide dismutase catalysis. FEBS Lett 184:237–239. https://doi.org/10.1016/0014-5793(85)80613-X
44. Lowry OH, Rosebrough NJ, Farr AL, Randall RJ (1951) Protein measurement with the Folin phenol reagent. J Biol Chem 193:265–275. https://doi.org/10.1016/S0021-9258(19)52451-6
45. Ryter SW, Alam J, Choi AMK (2006) Heme oxygenase-1/carbon monoxide: from basic science to therapeutic applications. Physiol Rev 86:583–650. https://doi.org/10.1152/PHYSREV.00011.2005
46. Amaral AU, Wajner M (2022) Pathophysiology of maple syrup urine disease: focus on the neurotoxic role of the accumulated branched-chain amino acids and branched-chain α-keto acids. Neurochem Int 157:105360. https://doi.org/10.1016/J.NEUINT.2022.105360
47. Strauss KA, Puffenberger EG, Carson VJ (2020) Maple syrup urine disease. In: Adam MP, Ardinger HH, Pagon RA, Wallace SE, Bean LJ, Mirzaa G, Amemiya A (eds) GeneReviews® [Internet]. University of Washington, Seattle (WA), pp. 1–33
48. Mescka CP, Guerreiro G, Donida B et al (2015) Investigation of inflammatory profile in MSUD patients: benefit of L-carnitine supplementation. Metab Brain Dis 30:1167–1174. https://doi.org/10.1007/S11011-015-9686-9
49. Scaini G, Tonon T, de Souza CFM et al (2016) Serum markers of neurodegeneration in maple syrup urine disease. MolNeurobiol 54:5709–5719. https://doi.org/10.1007/S12035-016-0116-8
50. Scaini G, Tonon T, Moura de Souza CF et al (2018) Evaluation of plasma biomarkers of inflammation in patients with maple syrup urine disease. J Inherit Metab Dis 41:631–640. https://doi.org/10.1007/S10545-018-0188-X
51. Boado RJ, Li JY, Nagaya M et al (1999) Selective expression of the large neutral amino acid transporter at the blood-brain barrier. Proc Natl Acad Sci U S A 96:12079–12084. https://doi.org/10.1073/PNAS.96.21.12079
52. Killian DM, Chikhale PJ (2001) Predominant functional activity of the large, neutral amino acid transporter (LAT1) isoform at the cerebrovasculature. Neurosci Lett 306:1–4. https://doi.org/10.1016/S0304-3940(01)01810-9
53. Sperringer JE, Addington A, Hutson SM (2017) Branched-chain amino acids and brain metabolism. Neurochem Res 42:1697–1709. https://doi.org/10.1007/S11064-017-2261-5
54. Ayala A, Muñoz MF, Argüelles S (2014) Lipid peroxidation: production, metabolism, and signaling mechanisms of malondialdehyde and 4-hydroxy-2-nonenal. Oxidative Med Cell Longev 2014:360438. https://doi.org/10.1155/2014/360438
55. Gaschler MM, Stockwell BR (2017) Lipid peroxidation in cell death. Biochem Biophys Res Commun 482:419–425. https://doi.org/10.1016/J.BBRC.2016.10.086
56. Dalle-Donne I, Rossi R, Giustarini D et al (2003) Protein carbonyl groups as biomarkers of oxidative stress. Clin Chim Acta 329:23–38. https://doi.org/10.1016/S0009-8981(03)00003-2
57. Levine RL, Williams JA, Stadtman EP, Shacter E (1994) [37] Carbonyl assays for determination of oxidatively modified proteins. Methods Enzymol 233:346–357. https://doi.org/10.1016/S0076-6879(94)33040-9
58. Kwon DH, Cha HJ, Lee H et al (2019) Protective effect of glutathione against oxidative stress-induced cytotoxicity in RAW 264.7 macrophages through activating the nuclear factor erythroid 2-related factor-2/heme oxygenase-1 pathway. Antioxidants 8:82. https://doi.org/10.3390/ANTIOX8040082
59. Vijayan V, Wagener FADTG, Immenschuh S (2018) The macrophage heme-heme oxygenase-1 system and its role in inflammation. Biochem Pharmacol 153:159–167. https://doi.org/10.1016/J.BCP.2018.02.010
60. Szabo IL, Kenyeres A, Szegedi A, Szollosi AG (2018) Heme oxygenase and the skin in health and disease. Curr Pharm Des 24:2303–2310. https://doi.org/10.2174/1381612824666180717155953
61. Pope SAS, Milton R, Heales SJR (2008) Astrocytes protect against copper-catalysed loss of extracellular glutathione. Neurochem Res 33:1410–1418. https://doi.org/10.1007/S11064-008-9602-3
62. Stewart VC, Stone R, Gegg ME et al (2002) Preservation of extracellular glutathione by an astrocyte derived factor with properties comparable to extracellular superoxide dismutase. J Neurochem 83:984–991. https://doi.org/10.1046/J.1471-4159.2002.01216.X
63. Halliwell B, Gutteridge JMC (2015) Antioxidant defenses synthesized in vivo. Free Radic Biol Med 77–152. https://doi.org/10.1093/ACPROF:OSO/9780198717478.003.0003
64. Arab JP, Roblero JP, Altamirano J et al (2019) Alcohol-related liver disease: clinical practice guidelines by the Latin American Association for the Study of the Liver (ALEH). Ann Hepatol 18:518–535. https://doi.org/10.1016/J.AOHEP.2019.04.005
65. Angelovski M, Hadzi-Petrushev N, Mitrokhin V et al (2023) Myocardial infarction and oxidative damage in animal models: objective and expectations from the application of cysteine derivatives. Toxicol Mech Methods 33:1–17. https://doi.org/10.1080/15376516.2022.2069530
66. Schoeps VA, Graves JS, Stern WA et al (2022) N-Acetyl cysteine as a neuroprotective agent in progressive multiple sclerosis (NACPMS) trial: study protocol for a randomized, double-blind, placebo-controlled add-on phase 2 trial. Contemp Clin Trials 122:106941. https://doi.org/10.1016/J.CCT.2022.106941
67. Santus P, Danzo F, Zuffi A et al (2022) Oxidative stress and viral infections: rationale, experiences, and perspectives on N-acetylcysteine. Eur Rev Med Pharmacol Sci 26:8582–8590. https://doi.org/10.26355/EURREV_202211_30395
68. Morris G, Anderson G, Dean O et al (2014) The glutathione system: a new drug target in neuroimmune disorders. Mol Neurobiol 50:1059–1084. https://doi.org/10.1007/S12035-014-8705-X
69. Pawlas N, Nierwińska K, Stolecka A et al (2009) Effects of N-acetylcysteine and ebselen on arachidonic acid release from astrocytes and neurons cultured in normoxic or simulated ischemic conditions. Pharmacol Rep 61:941–946. https://doi.org/10.1016/S1734-1140(09)70153-7
70. Rodriguez C, Mayo JC, Sainz RM et al (2004) Regulation of antioxidant enzymes: a significant role for melatonin. J Pineal Res 36:1–9. https://doi.org/10.1046/J.1600-079X.2003.00092.X
71. Malhotra S, Sawhney G, Pandhi P (2004) The therapeutic potential of melatonin: a review of the science. Medscape Gen Med 6:46
72. Tordjman S, Chokron S, Delorme R et al (2017) Melatonin: pharmacology, functions and therapeutic benefits. Curr Neuropharmacol 15:434–443. https://doi.org/10.2174/1570159X14666161228122115
73. Schaefer M, Hardeland R (2009) The melatonin metabolite N1-acetyl-5-methoxykynuramine is a potent singlet oxygen scavenger. J Pineal Res 46:49–52. https://doi.org/10.1111/J.1600-079X.2008.00614.X
74. Reiter RJ, Tan DX, Osuna C, Gitto E (2000) Actions of melatonin in the reduction of oxidative stress. A review. J Biomed Sci 7:444–458. https://doi.org/10.1007/BF02253360
75. Reiter RJ, Mayo JC, Tan DX et al (2016) Melatonin as an antioxidant: under promises but over delivers. J Pineal Res 61:253–278. https://doi.org/10.1111/JPI.12360
76. Hoppe JB, Frozza RL, Horn AP et al (2010) Amyloid-β neurotoxicity in organotypic culture is attenuated by melatonin: involvement of GSK-3β, tau and neuroinflammation. J Pineal Res 48:230–238. https://doi.org/10.1111/J.1600-079X.2010.00747.X

77. Manchester LC, Coto-Montes A, Boga JA et al (2015) Melatonin: an ancient molecule that makes oxygen metabolically tolerable. J Pineal Res 59:403–419. https://doi.org/10.1111/JPI.12267
78. Tan DX, Manchester LC, Esteban-Zubero E et al (2015) Melatonin as a potent and inducible endogenous antioxidant: synthesis and metabolism. Molecules 20:18886–18906. https://doi.org/10.3390/MOLECULES201018886
79. Wen J, Ariyannur PS, Ribeiro R et al (2016) Efficacy of N-acetylserotonin and melatonin in the EAE model of multiple sclerosis. J NeuroImmune Pharmacol 11:763–773. https://doi.org/10.1007/S11481-016-9702-9
80. Muhammad T, Ali T, Ikram M et al (2019) Melatonin rescue oxidative stress-mediated neuroinflammation/neurodegeneration and memory impairment in scopolamine-induced amnesia mice model. J NeuroImmune Pharmacol 14:278–294. https://doi.org/10.1007/S11481-018-9824-3
81. Shah SA, Khan M, Jo MH et al (2017) Melatonin stimulates the SIRT1/Nrf2 signaling pathway counteracting lipopolysaccharide (LPS)-induced oxidative stress to rescue postnatal rat brain. CNS Neurosci Ther 23:33–44. https://doi.org/10.1111/CNS.12588
82. Yarmohammadi F, Barangi S, Aghaee-Bakhtiari SH et al (2023) Melatonin ameliorates arsenic-induced cardiotoxicity through the regulation of the Sirt1/Nrf2 pathway in rats. BioFactors 49:620–635. https://doi.org/10.1002/BIOF.1934
83. Ali T, Hao Q, Ullah N et al (2020) Melatonin act as an antidepressant via attenuation of neuroinflammation by targeting Sirt1/Nrf2/HO-1 signaling. Front Mol Neurosci 13:96. https://doi.org/10.3389/FNMOL.2020.00096
84. Gan L, Johnson JA (2014) Oxidative damage and the Nrf2-ARE pathway in neurodegenerative diseases. Biochim Biophys Acta 1842:1208–1218. https://doi.org/10.1016/J.BBADIS.2013.12.011
85. Hauschild TC, Guerreiro G, Mescka CP et al (2019) DNA damage induced by alloisoleucine and other metabolites in maple syrup urine disease and protective effect of l-carnitine. Toxicol in Vitro 57:194–202. https://doi.org/10.1016/J.TIV.2019.03.007
86. Mescka CP, Wayhs CAY, Guerreiro G et al (2014) Prevention of DNA damage by l-carnitine induced by metabolites accumulated in maple syrup urine disease in human peripheral leukocytes in vitro. Gene 548:294–298. https://doi.org/10.1016/J.GENE.2014.07.051
87. Hol EM, Pekny M (2015) Glial fibrillary acidic protein (GFAP) and the astrocyte intermediate filament system in diseases of the central nervous system. Curr Opin Cell Biol 32:121–130. https://doi.org/10.1016/J.CEB.2015.02.004
88. Pekny M, Pekna M (2014) Astrocyte reactivity and reactive astrogliosis: costs and benefits. Physiol Rev 94:1077–1098. https://doi.org/10.1152/PHYSREV.00041.2013
89. Olivera-Bravo S, Barbeito L (2015) A role of astrocytes in mediating postnatal neurodegeneration in glutaric acidemia-type 1. FEBS Lett 589:3492–3497. https://doi.org/10.1016/J.FEBSLET.2015.09.010
90. Escartin C, Galea E, Lakatos A et al (2021) Reactive astrocyte nomenclature, definitions, and future directions. Nat Neurosci 24:312–325. https://doi.org/10.1038/s41593-020-00783-4
91. Janigro D, Mondello S, Posti JP, Unden J (2022) GFAP and S100B: what you always wanted to know and never dared to ask. Front Neurol 13:835597. https://doi.org/10.3389/FNEUR.2022.835597
92. Boggs JM, Rangaraj G, Heng YM et al (2011) Myelin basic protein binds microtubules to a membrane surface and to actin filaments in vitro: effect of phosphorylation and deimination. Biochim Biophys Acta 1808:761–773. https://doi.org/10.1016/J.BBAMEM.2010.12.016
93. Harauz G, Boggs JM (2013) Myelin management by the 18.5-kDa and 21.5-kDa classic myelin basic protein isoforms. J Neurochem 125:334–361. https://doi.org/10.1111/JNC.12195
94. Lee J, Gravel M, Zhang R et al (2005) Process outgrowth in oligodendrocytes is mediated by CNP, a novel microtubule assembly myelin protein. J Cell Biol 170:661–673. https://doi.org/10.1083/JCB.200411047
95. Fulton D, Paez PM, Campagnoni AT (2010) The multiple roles of myelin protein genes during the development of the oligodendrocyte. ASN Neuro 2:25–37. https://doi.org/10.1042/AN20090051
96. Martin JJ, Schlote W (1972) Central nervous system lesions in disorders of amino-acid metabolism: a neuropathological study. J Neurol Sci 15:49–76. https://doi.org/10.1016/0022-510X(72)90121-9
97. Menkes JH, Philippart M, Fiol RE (1965) Cerebral lipids in maple syrup disease. J Pediatr 66:584–594. https://doi.org/10.1016/S0022-3476(65)80122-6
98. Crome L, Dutton G, Ross CF (1961) Maple syrup urine disease. J Pathol Bacteriol 81:379–384. https://doi.org/10.1002/PATH.1700810209
99. Silberman J, Dancis J, Feigin I (1961) Neuropathological observations in maple syrup urine disease: branched-chain ketoaciduria. Arch Neurol 5:351–363. https://doi.org/10.1001/ARCHNEUR.1961.00450160001001
100. Kamei A, Takashima S, Chan F, Becker LE (1992) Abnormal dendritic development in maple syrup urine disease. Pediatr Neurol 8:145–147. https://doi.org/10.1016/0887-8994(92)90038-Z
101. Popa-Wagner A, Mitran S, Sivanesan S et al (2013) ROS and brain diseases: the good, the bad, and the ugly. Oxidative Med Cell Longev 2013:963520. https://doi.org/10.1155/2013/963520
102. Rosa L, Galant LS, Dall'Igna DM et al (2016) Cerebral oedema, blood–brain barrier breakdown and the decrease in Na+,K+-ATPase activity in the cerebral cortex and hippocampus are prevented by dexamethasone in an animal model of maple syrup urine disease. Mol Neurobiol 53:3714–3723. https://doi.org/10.1007/S12035-015-9313-0
103. Wessler LB, de Miranda RV, Bittencourt Pasquali MA et al (2019) Administration of branched-chain amino acids increases the susceptibility to lipopolysaccharide-induced inflammation in young Wistar rats. Int J Dev Neurosci 78:210–214. https://doi.org/10.1016/J.IJDEVNEU.2019.07.007